Title

Cold-stimulated brown adipose tissue activation is related to changes in serum metabolites relevant to NAD+ metabolism in humans

Journal

Cell Reports, 42(9)

ISSN

2639-1856

Authors

U-Din, Mueez

de Mello, Vanessa D

Tuomainen, Marjo

et al.

Publication Date

2023-09-01

DOI

10.1016/j.celrep.2023.113131

Cell Reports

Article

Cold-stimulated brown adipose tissue activation is related to changes in serum metabolites relevant to NAD$^+$ metabolism in humans

Graphical abstract

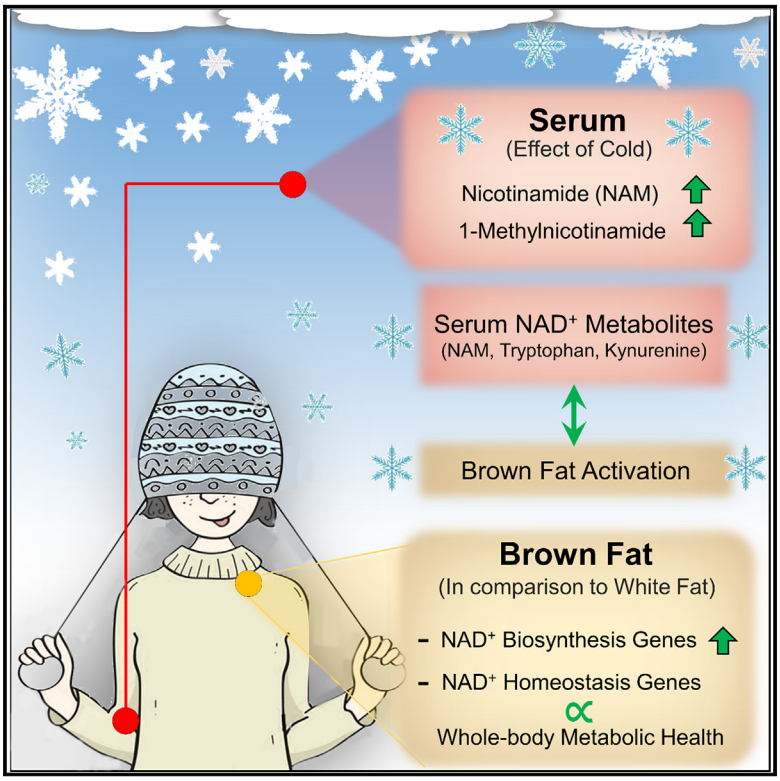

Highlights

- Cold induces a change in serum metabolites that are essential to NAD$^+$ metabolism
- Circulatory NAM, tryptophan, and kynurenine are linked to BAT activation during cold
- NAD$^+$ biosynthesis pathways are upregulated in BAT compared with WAT
- BAT NAD$^+$ biosynthesis is related to whole-body metabolic health

Authors

Mueez U-Din, Vanessa D. de Mello, Marjo Tuomainen, ..., Eija Pirinen, Kati Hanhineva, Kirsi A. Virtanen

Correspondence

kirsi.virtanen@utu.fi

In brief

U-Din et al. show that cold-stimulated BAT metabolism is linked to circulatory serum metabolites crucial for NAD$^+$ biosynthesis. In BAT, the pathways of NAD$^+$ biosynthesis, upregulated in comparison to WAT, are linked to thermogenic mechanisms and with whole-body metabolic health.

U-Din et al., 2023, Cell Reports *42*, 113131
September 26, 2023
https://doi.org/10.1016/j.celrep.2023.113131

CellPress

Cell Reports

CellPress
OPEN ACCESS

Article

Cold-stimulated brown adipose tissue activation is related to changes in serum metabolites relevant to NAD$^+$ metabolism in humans

Mueez U-Din,[1,2,23] Vanessa D. de Mello,[3,23] Marjo Tuomainen,[3] Juho Raiko,[1] Tarja Niemi,[4] Tobias Fromme,[5,6,7] Anton Klåvus,[3] Nadine Gautier,[8] Kimmo Haimilahti,[9,10] Marko Lehtonen,[11] Karsten Kristiansen,[12] John W. Newman,[13,14,15] Kirsi H. Pietiläinen,[16,17] Jussi Pihlajamäki,[3,18] Ez-Zoubir Amri,[8] Martin Klingenspor,[5,6,7] Pirjo Nuutila,[1,2,19] Eija Pirinen,[9,20,24] Kati Hanhineva,[3,21,22,24] and Kirsi A. Virtanen[1,2,3,18,19,25,*]

[1]Turku PET Centre, Turku University Hospital, Turku, Finland
[2]Turku PET Centre, University of Turku, Turku, Finland
[3]Department of Public Health and Clinical Nutrition, University of Eastern Finland, Kuopio, Finland
[4]Department of Surgery, Turku University Hospital, Turku, Finland
[5]Chair for Molecular Nutritional Medicine, Technical University of Munich, Freising, Germany
[6]EKFZ – Else Kröner Fresenius Center for Nutritional Medicine, Technical University of Munich, Freising, Germany
[7]ZIEL – Institute for Food & Health, Technical University of Munich, Freising, Germany
[8]Université Côte d'Azur, CNRS, Inserm, iBV, Nice, France
[9]Research Program for Clinical and Molecular Metabolism, Faculty of Medicine, University of Helsinki, 00290 Helsinki, Finland
[10]Research Program for Stem Cells and Metabolism, Faculty of Medicine, University of Helsinki, 00290 Helsinki, Finland
[11]Department of Pharmacy, University of Eastern Finland, Kuopio, Finland
[12]Department of Biology, University of Copenhagen, Copenhagen, Denmark
[13]Obesity and Metabolism Research Unit, USDA-ARS Western Human Nutrition Research Center, Davis, CA, USA
[14]West Coast Metabolomics Center, Davis Genome Center, University of California, Davis, Davis, CA 95616, USA
[15]Department of Nutrition, University of California, Davis, Davis, CA 95616, USA
[16]Obesity Research Unit, Research Program for Clinical and Molecular Metabolism, Faculty of Medicine, University of Helsinki, Helsinki, Finland
[17]Obesity Center, Abdominal Center, Helsinki University Hospital and University of Helsinki, Helsinki, Finland
[18]Department of Endocrinology and Clinical Nutrition, Department of Medicine, Kuopio University Hospital, Kuopio, Finland
[19]Department of Endocrinology, Turku University Hospital, Turku, Finland
[20]Research Unit for Internal Medicine, Faculty of Medicine, University of Oulu, 90220 Oulu, Finland
[21]Department of Life Technologies, Food Chemistry and Food Development Unit, University of Turku, Turku, Finland
[22]Department of Biology and Biological Engineering, Division of Food and Nutrition Science, Chalmers University of Technology, Gothenburg, Sweden
[23]These authors contributed equally
[24]These authors contributed equally
[25]Lead contact
*Correspondence: kirsi.virtanen@utu.fi
https://doi.org/10.1016/j.celrep.2023.113131

SUMMARY

Cold-induced brown adipose tissue (BAT) activation is considered to improve metabolic health. In murine BAT, cold increases the fundamental molecule for mitochondrial function, nicotinamide adenine dinucleotide (NAD$^+$), but limited knowledge of NAD$^+$ metabolism during cold in human BAT metabolism exists. We show that cold increases the serum metabolites of the NAD$^+$ salvage pathway (nicotinamide and 1-methylnicotinamide) in humans. Additionally, individuals with cold-stimulated BAT activation have decreased levels of metabolites from the *de novo* NAD$^+$ biosynthesis pathway (tryptophan, kynurenine). Serum nicotinamide correlates positively with cold-stimulated BAT activation, whereas tryptophan and kynurenine correlate negatively. Furthermore, the expression of genes involved in NAD$^+$ biosynthesis in BAT is related to markers of metabolic health. Our data indicate that cold increases serum tryptophan conversion to nicotinamide to be further utilized by BAT. We conclude that NAD$^+$ metabolism is activated upon cold in humans and is probably regulated in a coordinated fashion by several tissues.

INTRODUCTION

Impairment in brown adipose tissue (BAT) metabolism has been proposed to play a key role in the pathophysiology of obesity and multi-organ insulin resistance. Therefore, promoting BAT activation is considered a promising option to postpone or treat obesity and even metabolic disorders such as type 2 diabetes, due to its beneficial effects on measures of whole-body

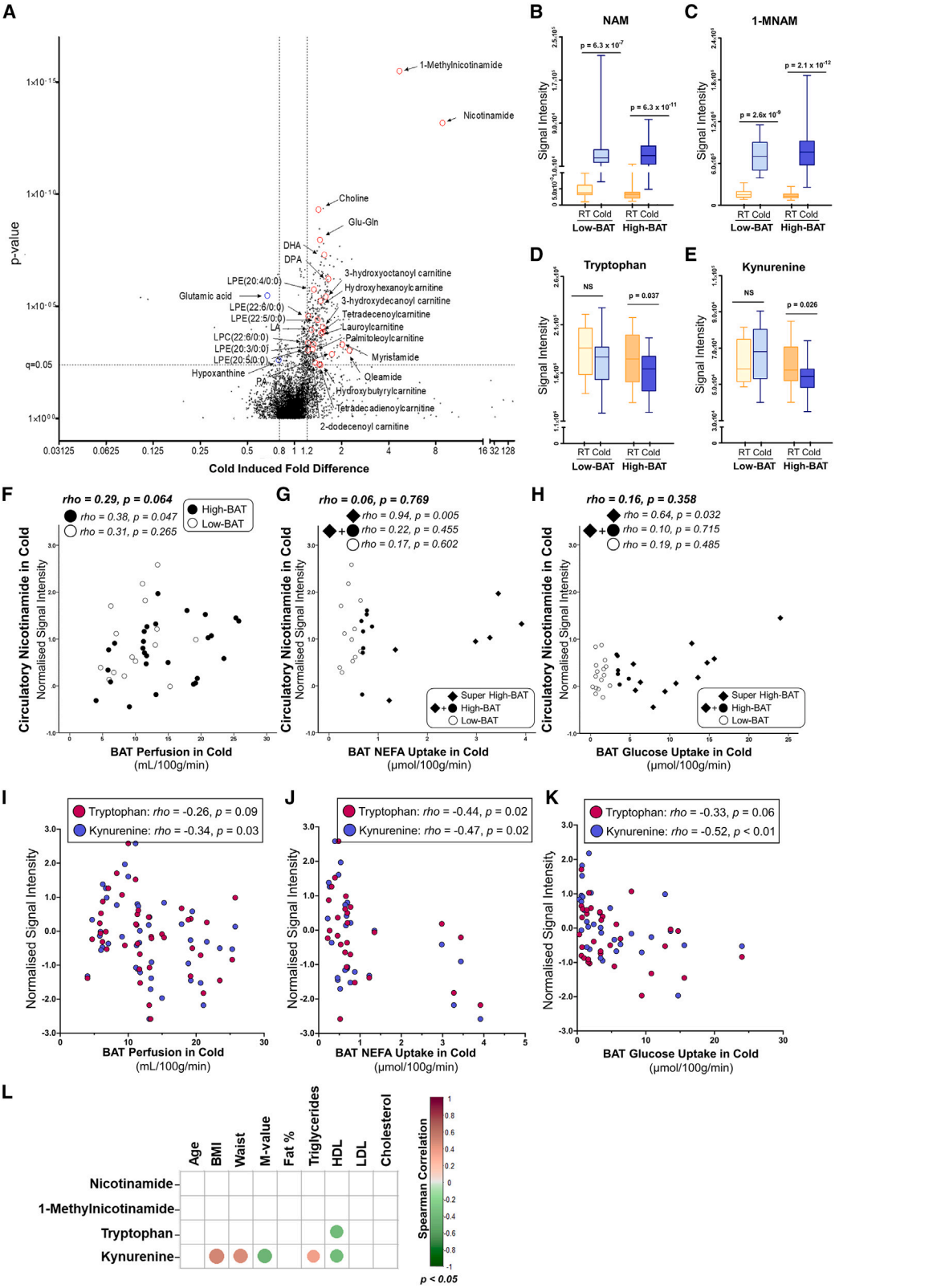

(legend on next page)

metabolic health, e.g., improved insulin sensitivity, plasma lipid profile, and body fat composition.[1–5] Once activated, BAT generates heat by uncoupling mitochondrial respiration via the action of uncoupling protein 1 (UCP1).[6] Repeated cold exposure or cold acclimation induces systemic metabolic health benefits in a BAT-activation-dependent manner.[7,8] However, owing to the uncomfortable nature of cold stress, this approach may result in lower compliance and feasibility. Thus, cold exposure is not a viable treatment option for many individuals. Hence, additional methods to activate BAT that mimic the molecular mechanisms of cold stress are currently under investigation.[9]

One indirect approach for activating BAT involves boosting energy and lipid metabolism with compounds that improve mitochondrial respiration. The most promising compounds for this purpose are those that increase intracellular levels of nicotinamide adenine dinucleotide (NAD^+), which is the central co-factor of mitochondrial energy conversion.[10] Based on rodent studies, an imbalance between NAD^+ bioavailability, consumption, and requirement for thermogenic respiration can potentially explain the decline in the metabolic capacity of BAT.[11,12] In line with this notion, NAD^+ depletion has been shown to occur in certain metabolic diseases, based on animal studies[13–15] and a few human studies.[16] However, limited information is available on the bioregulation and metabolism of NAD^+ in human BAT at room temperature and upon cold exposure. Nevertheless, the evidence from rodent studies has brought encouraging results showing that elevation in NAD^+ promotes mitochondrial function, BAT thermogenic activation, and an overall healthier metabolic phenotype.[10,17–20] In addition, *in vitro* norepinephrine-stimulated mitochondrial uncoupling in adipocytes derived from human BAT has been reported to be induced by an exogenous increase in NAD^+.[21]

In our present study, we first aimed to investigate the molecular signatures of the serum metabolome induced by cold exposure that may influence BAT metabolism. We also comprehensively examined whether the inter-individual variability in cold-induced detectable serum metabolites related to NAD^+ metabolism reflects cold-stimulated BAT metabolism as determined by positron emission tomography-computed tomography (PET-CT) imaging and whole-body systemic metabolic health in adult humans. Furthermore, to elucidate the bioregulation of NAD^+ in human BAT, we examined the molecular pathways involved in NAD^+ biosynthesis, transport, and consumption in comparison to white adipose tissue (WAT). Additionally, we investigated whether the inter-individual variation in the expression of genes involved in the cellular bioregulation of NAD^+ has a link to cold-stimulated BAT metabolism and markers of whole-body metabolic health in adult humans.

Further, we studied the effect of selected NAD^+ precursors on the intracellular NAD^+ levels and expression of NAD^+ biosynthetic genes and *UCP1* in human brite adipocytes. The results of this study therefore deepen our current understanding of the metabolism of NAD^+ and its regulation in human BAT and help identify targets to activate BAT to be used in further clinical experimental studies.

RESULTS

NAD^+-metabolism-related metabolites are the most upregulated serum metabolites during cold

We used non-targeted metabolomic profiling of fasting serum samples of healthy individuals that were lean or obese (Table S1). These subjects participated in previous acute cold-exposure studies at Turku PET Centre, Finland, where the focus has been to investigate the metabolism of BAT in various physiological states.[22–25] We studied serum samples from individuals exposed to cold, room temperature (RT), or both conditions. We observed that cold exposure caused large effects (false discovery rate [FDR] $p < 0.05$) on the serum metabolome when compared to RT (Figure 1A and Table S2). Cold-induced changes in many lipid species, acylcarnitines, and metabolites were related to both energy metabolism and amino acids (Table S2 and Figure 1A) in a manner similar to those observed in cold-exposed mice,[26] where acylcarnitines were increased in plasma. Higher acylcarnitine likely reflects free fatty acid mobilization due to cold-induced lipolysis, previously observed in response to cold.[22,24,27]

Interestingly, we identified NAD^+-metabolism-related metabolites, nicotinamide (NAM) and 1-methyl nicotinamide (1-MNAM), to be among those presenting the greatest differences between cold and RT exposures (Figure 1A). More specifically, NAM and 1-MNAM were the metabolites that exhibited the largest increase (approximately, 8-fold and 4-fold, respectively) during cold compared to RT (Figure 1A).

Figure 1. Serum metabolomics differences between room temperature and cold, and relation of NAD^+-metabolism-related metabolites with BAT metabolism and systemic metabolic health

(A) Volcano plot representation of metabolites detected in the serum. The dotted horizontal line represents the significance threshold (FDR $p < 0.05$) for the difference between signals in cold and room temperature (RT) exposures. DHA, docosahexaenoic acid; DPA, docosapentaenoic acid; LA, linoleic acid; LPC, lysophosphocholine; LPE, lysophosphoethanolamine; PA, palmitamide.

(B–E) Comparison of signal intensities of NAD^+-related metabolites in high-BAT and low-BAT individuals in RT in comparison with cold exposure. Boxes represent confidence intervals, the middle line represents the mean, and the error bars represent the range. Comparison of means was performed with unpaired Student's t test.

(F–H) Cross-sectional Spearman correlations (rho) of cold-induced fasting serum NAM (nicotinamide) and cold-stimulated BAT (F) Perfusion, (G) NEFA uptake, and (H) glucose uptake, according to BAT classification as high-BAT and low-BAT.

(I–K) Cross-sectional correlations of cold-induced fasting serum tryptophan and kynurenine with cold-stimulated BAT (I) perfusion, (J) NEFA uptake, and (K) glucose uptake.

(L) Cross-sectional correlations of NAD^+-related metabolites in cold exposure and baseline parameters of whole-body metabolic health. BMI, body mass index; M-value, whole-body insulin sensitivity measured with hyperinsulinemic-euglycemic clamp; Fat %, whole-body percentage of stored fat; HDL. high-density lipoprotein; LDL, low-density lipoprotein.

Information about the number of participants (n) in each analysis can be found in Figure S1.

Given that we were also able to identify *de novo* NAD^+-biosynthesis-related metabolites, tryptophan and kynurenine, via a non-targeted serum metabolomics approach, we next asked whether and how cold-induced differences in these four NAD^+-related metabolites (i.e., NAM, 1-MNAM, tryptophan, and kynurenine) were dependent on the degree of BAT activation. We first compared the circulatory levels of these four metabolites based on the response of BAT activation to cold, i.e., high-BAT and low-BAT activation. We classified the subjects as high-BAT or low-BAT based on substrate (glucose or non-esterified fatty acid [NEFA]) uptake determined by PET imaging, which are typical markers for cold-stimulated brown fat activation.[22,23,28–30] The classification was performed such that subjects in the high-BAT group had a glucose uptake rate of $\geq$3.0 μmol/100 g/min or NEFA uptake rate of $\geq$0.7 μmol/100 g/min after cold exposure, while the remaining participants were included in the low-BAT group.[22,23]

We found that the serum NAM and 1-MNAM levels were higher during cold in both high- and low-BAT individuals (Figures 1B and 1C) as compared with RT. However, cold-stimulated serum levels of neither NAM nor 1-MNAM were found to be different between high-BAT or low-BAT groups ($p = 0.20$ and $p = 0.98$, respectively, Figures 1B and 1C). Interestingly, serum levels of both tryptophan and kynurenine were significantly lower in high-BAT individuals in cold than at RT (Figures 1D and 1E), while temperature-dependent differences were not observed in these parameters in low-BAT individuals (Figures 1D and 1E). Cold-stimulated serum levels of both tryptophan and kynurenine were also lower in high-BAT subjects than in low-BAT subjects ($p = 0.029$ and $p = 0.00043$, respectively, Figures 1D and 1E). These findings imply that cold induces a rapid release of NAM into circulation while circulating tryptophan or kynurenine are likely directed for utilization in tissues in a BAT-activation-dependent manner.

Serum NAD^+-metabolism-related metabolites correlate with BAT activation

To further elucidate the relationship of circulatory NAM, tryptophan, and kynurenine with BAT metabolism, we also assessed correlations of cold-induced serum levels of these metabolites with cold-stimulated BAT substrate uptake and BAT blood perfusion. In addition to substrate uptake, BAT blood perfusion also reflects BAT activation.[23,31] In subjects in the high-BAT group, the cold-stimulated perfusion rate of BAT had a significant and positive relationship with cold-stimulated serum levels of NAM ($p = 0.047$), which was weakened when the whole population was considered ($p = 0.06$, Figure 1F). We observed no clear relationship between NAM and BAT substrate uptake rates in the whole cohort, nor were the relations significant when the subjects were grouped either as high-BAT or low-BAT (Figures 1G and 1H).

However, when we focused on the subjects with the highest cold-simulated BAT substrate uptake (either glucose uptake $\geq$5.0 μmol/100 g/min or NEFA uptake rate $\geq$1.0 μmol/100 g/min, termed super-high BAT in Figures 1G and 1H), cold-induced NAM showed a significant positive relationship with BAT substrate uptake rates (Figures 1G and 1H). When we analyzed the correlation of tryptophan and kynurenine with BAT parameters, we observed that cold-induced circulatory levels of tryptophan and kynurenine tended to inversely associate with cold-stimulated BAT blood perfusion, BAT NEFA uptake, and BAT glucose uptake in the whole cohort (Figures 1I–1K). Together, our findings suggest that cold-induced circulatory levels of NAM and the metabolites of the *de novo* NAD^+ biosynthesis pathway, tryptophan and kynurenine, have relevance to BAT metabolism and activation in humans.

Given that BAT metabolic activity has been linked to several indicators of whole-body metabolic health, including body adiposity,[23,25,32,33] we aimed to investigate whether the cold-induced serum levels of NAM, 1-MNAM, tryptophan, and kynurenine would be related to the metabolic phenotypes of the subjects (Figure 1L). However, in the case of NAM and 1-MNAM, except for a trend for whole-body fat percentage to be inversely correlated with NAM levels ($rho = -0.25$, $p = 0.05$), no other significant relationships were observed. In the case of tryptophan and kynurenine, we observed body mass index (BMI), waist circumference, and circulatory triglyceride levels to be directly related to the signal abundance for serum kynurenine (Figure 1L), while whole-body insulin sensitivity (M value) and serum high-density lipoprotein (HDL) levels were inversely related. The cold-induced serum tryptophan levels were in a relationship with both kynurenine ($rho = 0.51$; $p = 3.9 \times 10^{-5}$) and HDL circulatory levels (Figure 1L).

Overall, NAM and 1-MNAM scarcely relate to the subjects' metabolic profile for their systemic response to cold. In contrast, tryptophan and kynurenine, which were both lower in high-BAT than in low-BAT individuals under cold exposure and inversely related to BAT activity, seem to be more tightly related to subjects' degree of obesity, insulin sensitivity, and lipid profile.

NAD^+ biosynthesis and consumption pathways in BAT

Owing to the high metabolic activity of BAT compared to WAT,[34] the high requirement for intracellular NAD^+ levels can only be met with efficient NAD^+ biosynthesis in BAT. Mouse studies have shown that NAD^+ biosynthesis and consumption are likely higher in BAT than WAT,[35] but human data are lacking. To explore which metabolic pathways of NAD^+ biosynthesis and consumption are differentially regulated in human BAT and WAT, we investigated the expression of genes related to NAD^+ biosynthesis and consumption in samples of human BAT and WAT. In addition, we examined tryptophan (the essential amino acid involved in *de novo* NAD^+ biosynthesis) content in both adipose tissue (AT) types using metabolomics of tissue samples. Cellular biosynthesis of NAD^+ is attributed to several pathways: tryptophan degradation via the kynurenine pathway (*de novo*), nicotinic acid (NA) conversion via the Press-Handler pathway, and conversion of NAM and nicotinamide riboside (NR) to nicotinamide mononucleotide (NMN) via the salvage pathways.[36–38] The consumption of NAD^+ is mainly mediated by poly(ADP) ribose polymerases (PARPs), cluster of differentiation 38 (CD38), and sirtuins, which compete for intracellular NAD^+ bioavailability.[10]

We additionally examined whether the expression of NAD^+ biosynthetic and consumption genes was associated with BAT-activity-related parameters. These relationships could explain the inter-individual variability in BAT thermogenic

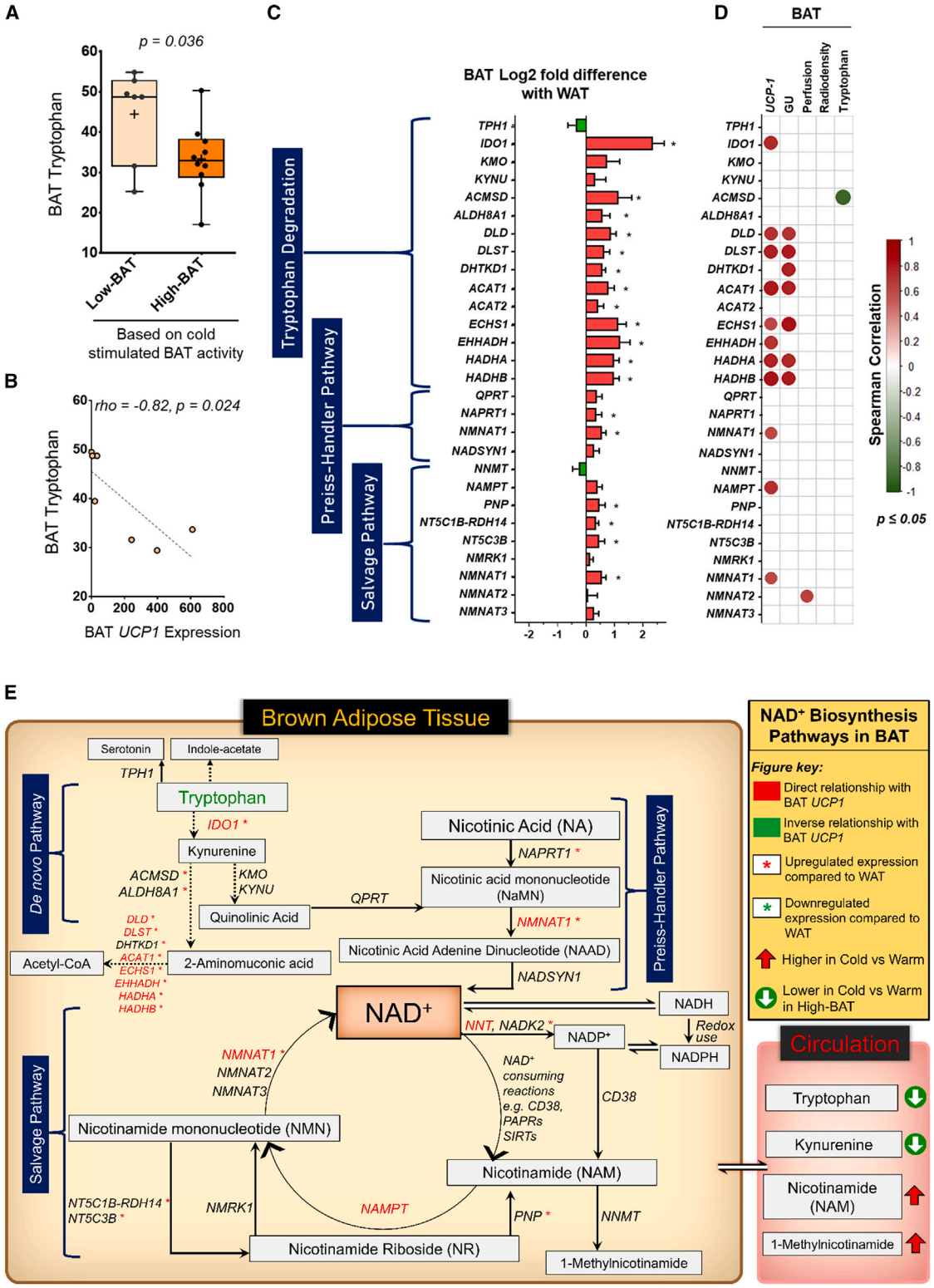

Figure 2. NAD⁺ biosynthesis pathways in BAT

(A) Comparison of BAT tryptophan content between high-BAT and low-BAT subjects. Box-and-whisker plot: box extends from the 25th to 75th percentiles, and whiskers show minimum to maximum value; mean value is marked with "+." p value shows the comparison of means using unpaired Student's t test.

(B) Spearman's correlation between BAT tryptophan content and BAT *UCP1* gene expression.

(legend continued on next page)

metabolism as determined by cold-stimulated PET-CT imaging measurements and *UCP1* expression in BAT. BAT samples were excised from the supraclavicular fat depot, and WAT samples were acquired from the subcutaneous neck fat depot. Owing to ethical considerations, the AT samples could not be acquired in the cold-stimulated state and were therefore collected under RT conditions.

De novo NAD$^+$ biosynthesis in BAT

To elucidate whether the favored routes for tryptophan catabolism differ between BAT and WAT, we statistically compared (using paired Student's t test or Wilcoxon's rank-sum test) the expression of genes involved in the metabolic pathways of tryptophan degradation, including the *de novo* NAD$^+$ biosynthesis pathway assessed with the KEGG (Kyoto Encyclopedia of Genes and Genomes) database tool[39,40] in these two tissues. Furthermore, we evaluated the relevance of BAT tryptophan-dependent NAD$^+$ biosynthesis to the thermogenic mechanism of BAT by analyzing the correlation of the expression of *de novo* pathway genes with BAT metabolic activity markers and BAT thermogenic gene *UCP1* mRNA levels.[6,41]

De novo biosynthesis of NAD$^+$ involves the conversion of tryptophan into NAD$^+$ in a multi-step process via indoleamine 2,3-dioxygenase 1 (IDO1) along the kynurenine pathway. Tryptophan can also be degraded toward the production of serotonin by tryptophan hydroxylase 1 (TPH1).[42] We found that BAT tryptophan content was significantly lower in high-BAT individuals compared to low-BAT individuals (Figure 2A), while there was no clear correlation between serum tryptophan and BAT tryptophan (rho = 0.13, p = 0.68), indicating that the differences observed in BAT (Figure 2A) may not be solely due to the differences in serum levels (Figure 1D). Further, *UCP1* expression of BAT was inversely related to BAT tryptophan content, indicating enhanced tryptophan tissue utilization upon BAT thermogenic activation (Figure 2B). We found that *IDO1* expression was significantly higher in BAT compared to WAT but there was no difference in *TPH1* expression between BAT and WAT (Figure 2C). Furthermore, the expression of *IDO1* was strongly associated with the expression of *UCP1* (Figure 2D). Thus, our results suggest that the degradation of tryptophan in BAT is favored toward kynurenine production in comparison to WAT, and that tryptophan degradation is important as a thermogenic mechanism of BAT.

The catabolism of kynurenine can lead to either production of acetyl-coenzyme A (acetyl-CoA) or NAD$^+$, with both molecules playing a fundamental role in the metabolic pathways of cellular respiration.[43] We found that the expression of several genes (*ACMSD*, *ALDH8A1*, *DLD*, *DLST*, *DHTKD1*, *ACAT1*, *ACAT2*, *ECHS1*, *EHHADH*, *HADHA*, and *HADHB*) in the metabolic pathway of the catabolic degradation of kynurenine leading to the production of acetyl-CoA was significantly higher in BAT than in WAT, and many of these genes were directly related to *UCP1* expression in BAT (Figures 2D and 2E). There were no differences in the expression of genes involved in the catabolism of kynurenine leading to the production of nicotinic acid mononucleotide (NaMN), a precursor of NAD$^+$ molecule, in BAT versus WAT. Thus, our data suggest that: (1) BAT has a superior capacity, compared to WAT, for catabolizing tryptophan toward kynurenine production; (2) in BAT, in comparison to WAT, kynurenine is likely channeled toward the production of acetyl-CoA rather than NAD$^+$; and (3) tryptophan degradation is directly linked with BAT thermogenesis.

Preiss-Handler pathway of NAD$^+$ biosynthesis in BAT

We further analyzed the expression of genes involved in the other pathways of NAD$^+$ production in BAT to elucidate the main NAD$^+$ biosynthetic mechanisms in BAT compared to WAT. In the Preiss-Handler pathway, the expression of genes involved in the conversion of NA (commonly referred to as niacin or vitamin B3) to NaMN, and further from NaMN to NA adenine dinucleotide (*NAAD*), *NAPRT1*, and *NMNAT1*, respectively, were significantly higher in BAT than in WAT. The expression of *NMNAT1*, but not *NAPRT1*, correlated positively with the expression of *UCP1*. There was no significant difference between the expression of other isoforms of NMNATs, i.e., *NMNAT2* and *NMNAT3*. Additionally, there was no significant difference in the expression of *NADSYN1*, the gene involved in the conversion of NAAD to NAD$^+$ (Figure 2C). Because *NAPRT1* is the key rate-limiting enzyme involved in metabolizing NA,[44] it can be inferred from our data that the Preiss-Handler pathway is upregulated in BAT compared to WAT, and that metabolism of food-derived NA might occur at higher rates in BAT than in WAT.

Salvage pathways of NAD$^+$ biosynthesis in BAT

When assessing salvage pathways in BAT, we found that the expression of the rate-limiting gene[45] *NAMPT* was not significantly upregulated in BAT (compared to the paired WAT, Figure 2C). Interestingly, the expression of *NAMPT* was directly related to the expression of *UCP1*, showing that *NAMPT* associates with BAT thermogenic activity in humans (Figure 2D). The expression of the gene responsible for conversion of NR to NMN, *NMRK1*, was not different in BAT compared to WAT, while the expression of the other isoform of *NMRK*, *NMRK2*, was not

(C) Log_2 fold difference of the expressions of the genes involved in NAD$^+$ biosynthesis pathways in BAT in comparison to WAT. Comparison of the means has been done with the paired Student's t test for normally distributed data or Wilcoxon's rank-sum test for the non-normally distributed datasets. *p $\leq$ 0.05. Data are presented as mean ± SEM.

(D) Relationship between the expressions of genes in BAT involved in NAD$^+$ biosynthesis pathways in comparison to BAT metabolic characteristics, i.e., *UCP1* expression, cold-stimulated glucose uptake (GU), cold-stimulated tissue perfusion, cold-stimulated tissue radiodensity, and tryptophan content. The relationships reaching statistical significance at a p value of $\leq$0.05 are shown.

(E) Graphical illustration of NAD$^+$ biosynthesis pathways in BAT in conjunction with the expression of genes in BAT involved in these synthesis pathways in comparison to WAT, and the relationship of these genes with the expression of BAT thermogenic gene (*UCP1*). Moreover, the cold-induced response of circulatory metabolites related to NAD$^+$ metabolism is illustrated. All the mentioned genes in the figure were evaluated for differences with WAT gene expression and correlation with BAT *UCP1* expression.

Information about the number of participants (n) in each analysis can be found in Figure S1.

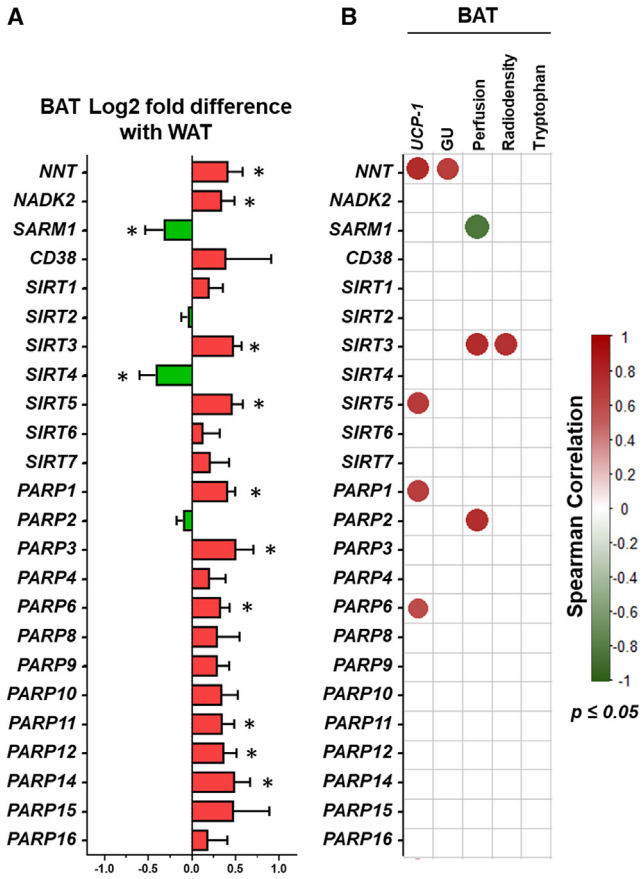

Figure 3. NAD$^+$ consumption pathways in BAT

(A) Log_2 fold difference of the expressions of the genes involved in NAD$^+$ consumption in BAT in comparison to WAT. Comparison of the means has been done with the paired Student's t test for normally distributed data or Wilcoxon's rank-sum test for the non-normally distributed datasets. *p ≤ 0.05. Data are presented as mean ± SEM.

(B) Relationship between the expressions of genes in BAT involved in NAD$^+$ consumption in comparison to BAT metabolic characteristics, i.e., *UCP1* expression, cold-stimulated glucose uptake (GU), cold-stimulated tissue perfusion, cold-stimulated tissue radiodensity, and tryptophan content. Spearman's correlations reaching statistical significance at a p value of ≤0.05 are shown.

Information about the number of participants (n) in each analysis can be found in Figure S1.

detected in BAT. The expression of *NMNAT1*, the gene encoding the enzyme responsible for conversion of NMN to NAD$^+$, was found to be upregulated in BAT versus WAT and positively correlated with *UCP1* expression. However, it should be noted that NMNAT1 also has relevance in the Preiss-Handler pathway, and the conclusion that NMN is solely converted to NAD$^+$ may not be entirely accurate. The expression of the gene responsible for converting NR to NAM, purine nucleoside phosphorylase (*PNP*), was found to be higher in BAT (Figure 2C) than in WAT, thus suggesting a higher capacity for conversion of NR to NAM in BAT than in WAT. There were no significant correlations between the expression of *UCP1* and the expression levels of *NRK1* and *PNP*. Together, these data suggest that most of the salvage pathway genes are expressed at a similar level in human BAT and WAT, but upon cold activation, BAT NAD$^+$ biosynthesis likely occurs via NAMPT-mediated mechanism in the salvage pathway in humans.

NAD$^+$ consumers in BAT

Given that intracellular NAD$^+$ availability depends not only on NAD$^+$ biosynthesis capacity but also on the rate of NAD$^+$ consumption, we investigated the expression of the genes encoding proteins involved in the consumption of NAD$^+$. Our data showed no differences in the expression of *CD38* between BAT and WAT (Figure 3A), suggesting that *CD38*-mediated NAD$^+$ consumption may not be contributing to the differences of intracellular NAD$^+$ between BAT and WAT. Our finding is in line with the results in mice reported by Benzi et al.[19] However, while our dataset does not reveal how cold may affect *CD38* mediated NAD$^+$ consumption, the data in mice suggest that cold exposure reduces *CD38* expression, which may still be a key mechanism leading to increased BAT NAD$^+$ levels during cold exposure.[19] Among the PARP family, we found that the expression of *PARP1*, *PARP3*, *PARP6*, *PARP11*, *PARP12*, and *PARP14* was upregulated in BAT compared to WAT (Figure 3A). The expression of *PARP5a*, *PARP5b*, and *PARP7* was not detected in BAT, contrary to the findings in rodents.[18] The main isoform, *PARP1*, and also *PARP6*, had a direct relationship with *UCP1* expression in BAT (Figure 3B). This implies that BAT with greater thermogenic capacity also expresses PARP1, responsible for mitigating DNA damage, a potential consequence of elevated free radicals in BAT due to its higher oxidative capacity relative to WAT.[34] Interestingly, *PARP1* gene ablation improves BAT thermogenic activity in mice,[18] and this is likely due to elevated cellular NAD$^+$ content. We found a relationship between the expressions of *PARP2* and cold-stimulated BAT perfusion, an indicator of BAT oxidative metabolism.[34] As a whole, our data demonstrated that the expression of the main *PARP* isoform, *PARP1*, and approximately 80% of the isoforms of this family have higher expression in human BAT than in WAT, while BAT *PARP1* gene expression is linked to BAT thermogenesis in humans.

Sirtuins are the key regulators of mitochondrial metabolism that use NAD$^+$ as a substrate for deacylation reactions.[46] We found that among the sirtuin family, the expression of mitochondrial sirtuins *SIRT3* and *SIRT5* were upregulated in BAT while the expression of mitochondrial *SIRT4* was downregulated in comparison to WAT (Figure 3A). The expression of *SIRT5* in BAT was also in direct relationship with the expression of *UCP1*, and the expression of *SIRT3* was in direct relationship with cold-stimulated BAT perfusion and radiodensity. *SIRT3*, localized on the inner mitochondrial membrane, participates in UCP1-mediated thermogenic respiration in BAT, and *in vitro* data suggest that it is necessary for BAT function, particularly lipid handling and mitochondrial respiration[47]; however, adipose-specific SIRT3 knockout data remain equivocal in this regard.[48,49] The protein encoded by *SIRT5* is involved in succinylation and malonylation of key metabolic enzymes in mitochondria and plays a role in promoting BAT metabolism.[50] In contrast, *SIRT4* is involved in repressing mitochondrial fatty acid oxidation and promoting lipid anabolism,[51] the latter of which is a dominant feature of WAT rather than BAT.

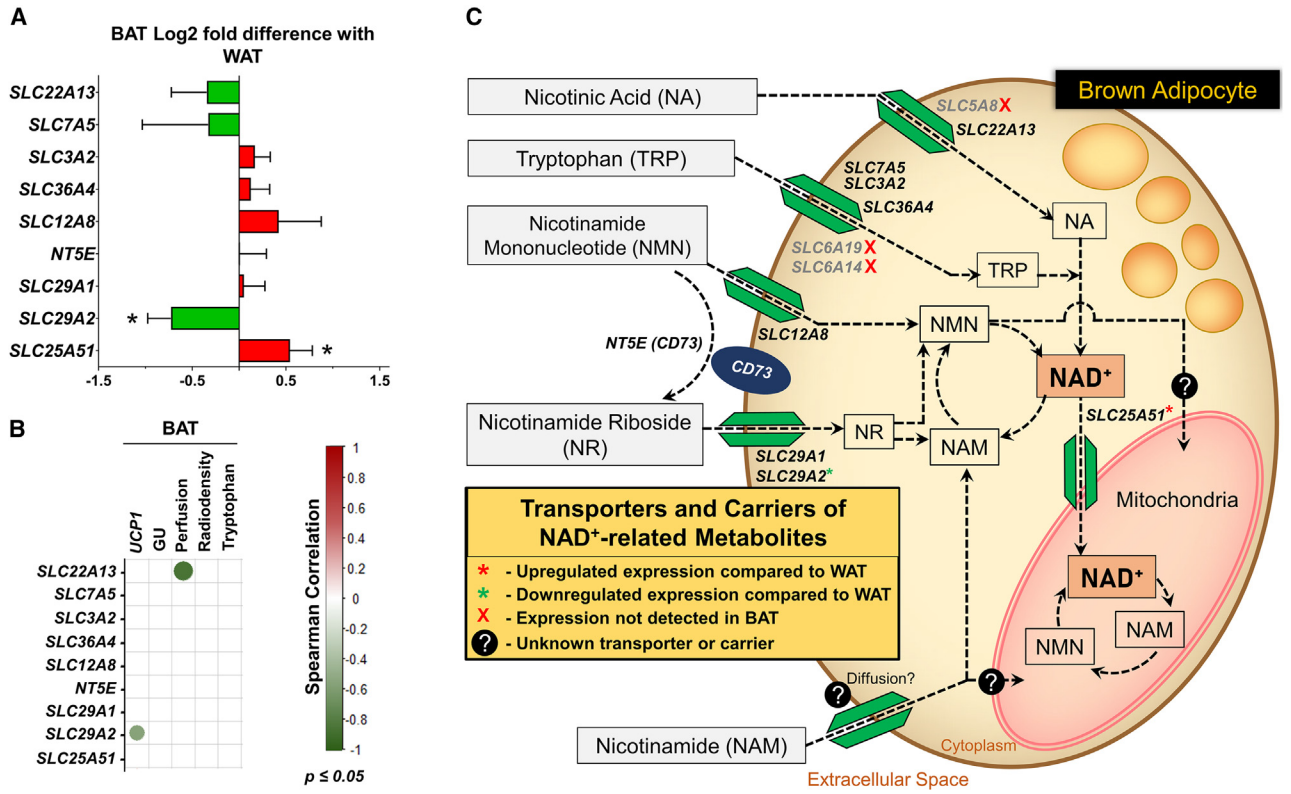

Figure 4. Transporter and carriers of NAD$^+$-related metabolites in BAT

(A) Log_2 fold difference of the expressions of the genes involved in the cellular uptake and transport of NAD$^+$-precursor molecules in BAT in comparison to WAT. Comparison of the means has been done with the paired Student's t test for normally distributed data or Wilcoxon's rank-sum test for the non-normally distributed datasets. *p $\leq$ 0.05. Data are presented as mean ± SEM.

(B) Relationship between the expressions of genes in BAT involved in the cellular uptake and transport of NAD$^+$-precursor molecules and metabolic characteristics of BAT, i.e., *UCP1* expression, cold-stimulated glucose uptake (GU), cold-stimulated tissue perfusion, cold-stimulated tissue radiodensity, and tryptophan content. Spearman's correlations reaching statistical significance at a p value of $\leq$0.05 are shown.

(C) Graphical representation of the transporter and carriers of NAD$^+$-related metabolites in a brown adipocyte, in conjunction with the findings in (A).

Information about the number of participants (n) in each analysis (data shown in A and B) can be found in Figure S1.

These results should be seen, however, in the context that typically mRNA expression of sirtuins does not correlate with enzyme activities.[46] Nevertheless, we clearly observed a differential expression of mitochondrial sirtuin genes in BAT in comparison to WAT and found relationships of sirtuins with markers of BAT metabolic activity.

Gene expression of transporter and carriers of NAD$^+$-related metabolites in BAT

Cellular-membrane-bound transporter proteins and molecular carriers play a crucial role in the regulation of the availability of key metabolites for cellular reactions. Recent data have emerged suggesting that certain transporters and carriers of NAD$^+$ precursor molecules play a crucial role in maintaining cellular NAD$^+$ homeostasis.[52,53] However, the findings are still somewhat controversial. Despite this, we compared the expression of genes encoding the transport receptors and carriers of NAD$^+$-related metabolites in BAT versus WAT.

Tryptophan has been suggested to enter cells through the neutral or proton-coupled amino acid transporters *SLC7A5*[54] and *SLC36A4*.[55] There were no differences in the expression of these genes between BAT and WAT (Figure 4A). The BAT tryptophan concentration was also not associated with the expression of these genes (Figure 4B). Regarding other potential tryptophan transporters in BAT, we did not detect the expression of the tryptophan-like amino acid transporters *SLC6A19* and *SLC6A14*, which are tryptophan-like amino acid transporters in several tissues,[56,57] in either AT type.

Cellular uptake of NA has been reported to be via *SLC5A8* and *SLC22A13*.[58,59] We did not detect the expression of *SLC5A8* in BAT. The expression of *SLC22A13* was detected, but it was not different from that of WAT (Figure 4A). The *SLC12A8* gene encodes a specific transporter of nicotinamide mononucleotide (NMN) in cells.[52] The expression of this gene was detected in BAT, although it was not statistically different from the corresponding WAT expression (Figure 4A). NMN is converted to NR extracellularly through the presence of protein on the cellular membrane encoded by *NT5E*. In BAT, expression of *NT5E* was detected, but the expression was not different from that in WAT.

SLC29A1 and *SLC29A2* encode the transporters of NR; the expression of both was detected in BAT. The expression of *SLC29A2* was significantly higher in WAT than in BAT. It is

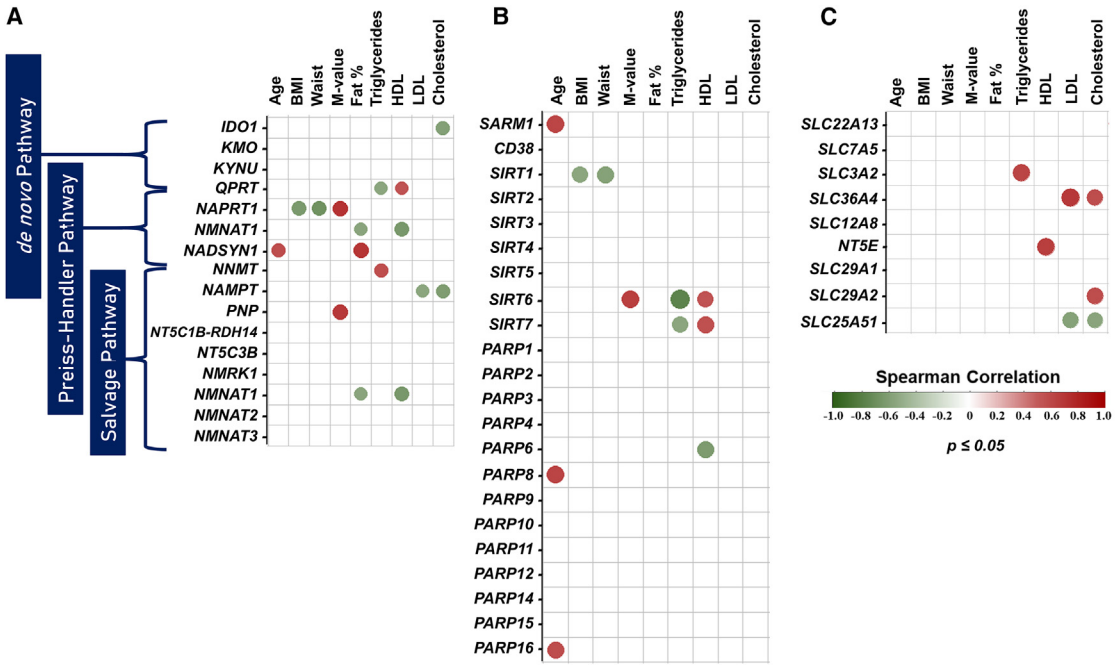

Figure 5. Whole-body metabolic health and NAD$^+$ biosynthesis, consumption, and transport genes in BAT

Spearman's correlations between the expressions of genes in BAT involved in (A) NAD$^+$ biosynthesis, (B) NAD$^+$ consumption, and (C) the cellular uptake and transport of NAD$^+$-precursor molecules with systemic metabolic health measures. The relationships reaching statistical significance at a p value of ≤0.05 are shown. Information about the number of participants (n) in each analysis can be found in Figure S1.

unclear whether a specific transport system exists for the cellular uptake of NAM in BAT. Previously it has been suggested that cellular NAM uptake in other tissues occurs via facilitated diffusion.[60,61] Recent studies have indicated that *SLC25A51* mediates the transport of NAD$^+$ synthesized in the cytoplasm to the mitochondria.[52,62,63] According to our data, the expression of *SLC25A51* was upregulated in BAT compared to WAT (Figure 4A), and there was a strong trend for a direct relationship between expressions of BAT *SLC25A51* and *UCP1* (rho = 0.51, p = 0.05) and of BAT expression of *SLC25A51* with BAT cold-induced glucose uptake (rho = 0.52, p = 0.10). This indicates a higher presence of this NAD$^+$ mitochondrial transport protein in BAT than in WAT, with possible relevance to the thermogenic mechanism in BAT.

The uptake of NMN into the mitochondria is another route for mitochondrial NAD$^+$ production via the salvage pathway, and it is considered to be the dominant precursor of NAD$^+$ production within mitochondria.[64,65] However, the exact mechanism of NMN uptake from the cytosol to mitochondria is unclear. Overall, based on these findings, there are no clear differences in the expression of the transporters of NAD$^+$ precursors between BAT and WAT, implying that all NAD$^+$ precursors can equally enter the white and brown adipocytes for NAD$^+$ biosynthesis.

Whole-body metabolic health and expression of genes involved in NAD$^+$ biosynthesis, consumption, and transport in BAT

Because BAT is suggested to be an organ that may be involved in the regulation of whole-body metabolic health, we examined the relationships of the expression of genes involved in NAD$^+$ biosynthesis, consumption, and transport in BAT with systemic markers of metabolic health (whole-body insulin sensitivity and plasma lipid profile) and markers of body adiposity (BMI, waist circumference, and whole-body fat percentage) (Figures 5A–5C). The markers of body adiposity were inversely related to the expression of *NAPRT1*, *NMNAT1*, and *SIRT1*, and directly related to *NADSYN1*. The whole-body insulin sensitivity (M value) was directly related to *NAPRT1*, *PNP*, and *SIRT6*. The measures of lipidemia (plasma triglycerides, cholesterol, low-density lipoprotein, and HDL) were related to the expression of *NMNAT1*, *NAMPT*, *NNMT*, *QPRT*, *SIRT6*, *SIRT7*, *PARP6*, *SLC2A2*, *SLC36A4*, *NT5E*, *SLC29A2*, and *SLC25A51*. Together, based on these findings, it can be inferred that the genes encoding proteins crucial for regulating cellular NAD$^+$ bioavailability in BAT are linked to systemic metabolic health.

Acute exposure to NAM and tryptophan on human brite adipocytes

We lastly asked whether exogenously administered NAM and tryptophan could affect NAD$^+$ levels and expression of genes involved in NAD$^+$ biosynthesis and thermogenesis in human brite adipocytes. In our *in vitro* experiments, we subjected human brite adipocytes acutely for 6 h to either NAM or tryptophan. We used two concentrations of these compounds, either 0.03 mM or 0.1 mM, based on a previous study using another NAD$^+$ precursor, NR, in human brite adipocytes.[21] Acute exposure to NAM (0.1 mM) significantly increased the intracellular NAD$^+$ concentration (Figure 6A), and this was associated with

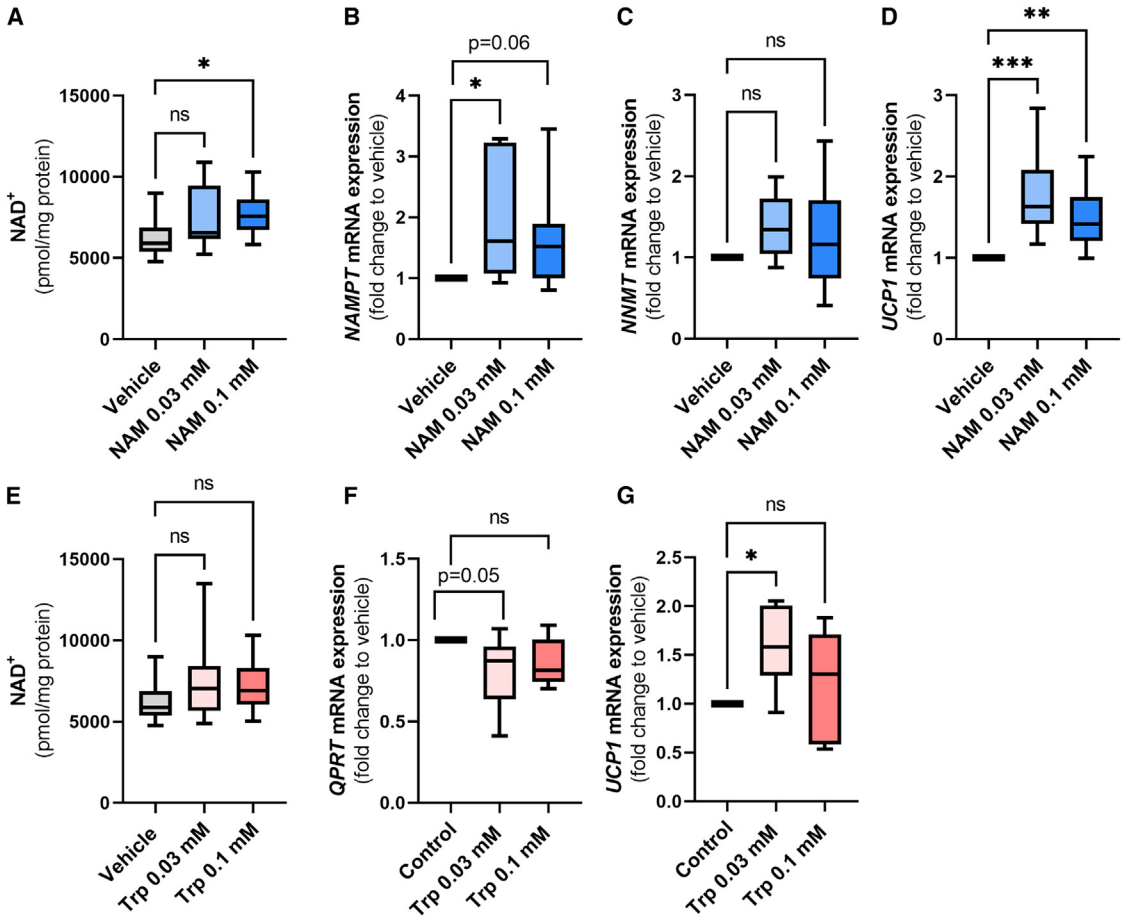

Figure 6. Exposure to nicotinamide and tryptophan in human brite adipocytes

(A–D) Effect of acute nicotinamide (NAM) treatment on intracellular NAD^+ concentration (vehicle, n = 8; NAM, n = 10) and the mRNA expression of *NAMPT* (vehicle, n = 10; NAM 0.03 mM, n = 6; NAM 0.1 mM, n = 10), *NNMT* (vehicle, n = 10; NAM 0.03 mM, n = 5; NAM 0.1 mM, n = 8), and *UCP1* (vehicle, n = 10; NAM 0.03 mM, n = 7; NAM 0.1 mM, n = 10) in human brite adipocytes.

(E–G) Effect of acute tryptophan (Trp) treatment on intracellular NAD^+ concentration (vehicle, n = 8; Trp, n = 10) and mRNA expression of *QPRT* (all groups, n = 6) and *UCP1* (all groups, n = 6) in human brite adipocytes. Statistical analysis was performed with one-way ANOVA with Fisher's LSD post hoc test for normally distributed data and with Kruskal-Wallis test with uncorrected Dunn's post hoc test for non-normally distributed data. *p < 0.05, **p < 0.01, ***p < 0.001; ns, not significant. Box-and-whisker plot: box extends from the 25th to 75th percentiles, and whiskers show minimum to maximum value; the mean value is marked with a line.

a trend for elevated expression of *NAMPT*, the NAM metabolizing NAD^+ biosynthetic gene (Figure 6B). In response to NAM treatment, there was no concurrent upregulation in the expression of *NNMT* that diverts NAM from NAD^+ biosynthesis (Figure 6C). Interestingly, acute exposure to NAM also increased *UCP1* expression (Figure 6D), demonstrating a direct link between the salvage pathway for NAD^+ biosynthesis and the UCP1-dependent thermogenic pathway in brite adipocytes. Exposure to tryptophan with any of the used concentrations did not elicit a response to the intracellular NAD^+ concentration in human brite adipocytes (Figure 6E), with no concurrent effect on *QPRT*, the rate-limiting gene in the *de novo* pathway of NAD^+ biosynthesis (Figure 6F). Interestingly, there was a significant increase in *UCP1* expression with the lowest dose of tryptophan (0.03 mM) (Figure 6G). This finding is in line with our earlier results (*de novo* NAD^+ biosynthesis in BAT) showing that tryptophan has a link to BAT thermogenic metabolism, although this is not pertinent to NAD^+ *de novo* biosynthesis. Collectively, these results confirmed that NAM and tryptophan have relevance to thermogenic metabolism in human brown adipocytes.

DISCUSSION

Based on mouse studies, cold exposure activates NAD^+ metabolism in BAT, reflecting the higher demand of NAD^+ for thermogenic metabolism in cold-stimulated BAT.[11] In humans, limited data are available on how NAD^+ metabolism is regulated in the supraclavicular BAT at RT and upon cold exposure. Our study addresses this important knowledge gap by analyzing cold-induced changes in serum metabolites and their relationship with the *in vivo* metabolic parameters of BAT and the expression of genes representing pathways that are central to NAD^+

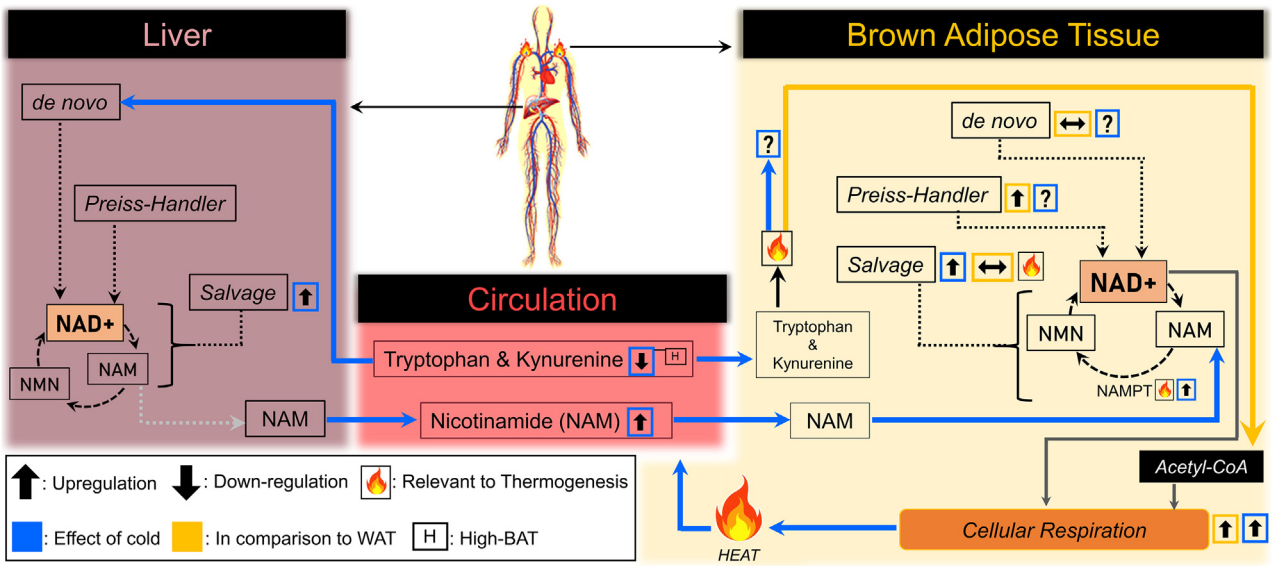

Figure 7. The proposed mechanism fulfilling intracellular NAD$^+$ requirements in human BAT, particularly during cold-induced thermogenesis

Liver releases NAM into the circulation in response to cold, which is taken up by BAT to be used for NAD$^+$ production via NAMPT in the salvage pathway. Concomitantly, decreased levels of kynurenine and tryptophan in the circulation found in individuals with high cold-stimulated BAT metabolism denote their utilization in liver for *de novo* synthesis of NAD$^+$ or in BAT for *de novo* synthesis of acetyl-CoA and/or NAD$^+$ upon cold-stress condition.

bioregulation in the supraclavicular BAT depots in adult humans. In addition, the effect of acute exposure to NAM and tryptophan on NAD$^+$ and thermogenic metabolism was evaluated in human brite adipocytes. Based on our findings and those of others, we propose a model of NAD$^+$ bioregulation in human BAT that is supported by the liver, particularly during hypermetabolic cold-stress conditions (Figure 7).

One of our key findings is that cold stimulation resulted in higher circulating levels of NAM and 1-MNAM in humans. NAM is a vitamin B3 form that is used for NAD$^+$ biosynthesis via the salvage pathway in peripheral tissues and is also the end product of several intracellular NAD$^+$ consumption reactions mediated by CD38 and PARPs.[66] In contrast, 1-MNAM is a degradation product of NAM that is eliminated via urine.[67,68,69] In mammals including humans, NAM is obtained via the diet, but it can also be biosynthesized from diet-derived tryptophan in the liver.[70] The secreted NAM in the circulation is taken up by other tissues for the synthesis of NAD$^+$ via NAMPT in the salvage pathway. Our findings invoke the question of what was the source of circulating NAM and 1-MNAM during cold exposure. It is plausible that NAD$^+$ consumption reactions in the blood cells, for example via SIRTs, CD38, and PARPs, contributed to the elevated levels of circulating NAM and 1-MNAM in our study.[71,72] However, it is tempting to speculate that the liver may be the major organ responsible for the cold-induced elevation in circulatory NAM, as rodent studies have shown the liver to release tryptophan-derived NAM for use in other tissues.[36] Consequently, NAM would then be taken up by BAT due to higher cellular NAD$^+$ demand to support thermogenic respiration (as suggested in Figure 7). In addition, supplementation with NAD$^+$ precursors has been reported to stimulate BAT thermogenic activity in mice.[11,73,74] These findings raise the question of whether the exogenous supplementation with NAM or other NAD$^+$ precursor vitamin B3 forms known to be degraded to NAM could be used as a means to stimulate human BAT activity. Interestingly, NR induced norepinephrine-stimulated mitochondrial uncoupling in adipocytes derived from human BAT after a 24-h treatment.[21] In the same study, however, the clinical trial with NR supplementation failed to detect BAT activation after 6 weeks of treatment.[21] There could be several reasons why *in vitro* and *in vivo* studies showed different outcomes upon NR supplementation. The dose and the duration of the treatment differed, and the degree of degradation of NR to NAM varies between *in vitro* and *in vivo* as well as the capacity of NR to elevate intracellular NAD$^+$ levels. Also, the study by Nascimento et al.[21] examined *in vivo* BAT metabolism during cold stimulation, and it is plausible that the hypermetabolic effect of cold activation in BAT may have masked the effect of NR supplementation, which may have been present during the basal metabolic state. Therefore, further studies are needed to aid understanding of whether NAM and NAD$^+$ boosting strategies can stimulate BAT activity in humans, not merely under cold stimulation but also in other physiological states (e.g., fasting and postprandial).

Further support for the idea that cold-stimulated BAT utilizes tryptophan-derived NAM via the salvage pathway comes from our observation that BAT thermogenic capacity, assessed on the basis of *UCP1* expression, was linked to the expression of *NAMPT* (Figure 2D). In line with our findings, gene and protein expression of *NAMPT* in the human supraclavicular AT (the most common location for the existence of human BAT in adults) has been shown to increase during cold exposure.[11] In mice, cold-induced upregulation of *NAMPT* expression in BAT[11,19] has been observed along with increased NAD$^+$ levels and NAD$^+$ metabolites involved in the salvage pathway, including

NAM.[11] In agreement, we observed that acute NAM treatment elevated intracellular NAD^+ levels and expression of *NAMPT* and *UCP1* in human brite adipocytes. Overall, our data suggest that hepatic NAM release to the circulation, and its utilization via the salvage pathway for NAD^+ biosynthesis, is likely functional and crucial in cold-activated BAT metabolism in humans (Figure 7).

Tryptophan is an essential amino acid derived from the diet to produce protein. In liver, tryptophan is mostly used for the synthesis of kynurenine, accounting for approximately 90% of tryptophan catabolism, while only 3% of dietary tryptophan is used for serotonin synthesis.[75–77] The observed decrease in serum tryptophan and kynurenine in response to cold was the most prominent phenomenon in those individuals with high-BAT activation. Given that animal studies suggest that the utilization of dietary tryptophan for the biosynthesis of NAD^+ and subsequent conversion to NAM takes place in the liver,[70,76] we propose that cold-induced hepatic tryptophan utilization may be the key factor explaining the decline in circulating tryptophan observed in our study (Figure 7). Although there is no direct evidence of increased hepatic utilization of tryptophan and kynurenine resulting in their decrease in circulation upon cold exposure in humans or mice, cold-stimulated BAT of mice has presented an increase in hepatic gene expression and activity of tryptophan-2,3-dioxygenase (TPO), suggesting an enhanced tryptophan catabolism in liver toward kynurenine production under this hypermetabolic condition.[78] The increase in the hepatic tryptophan pool per se has been shown to increase TPO activity, due to higher blood flow toward the liver caused by peripheral vasoconstriction resulting from cold exposure.[79,80] In humans, BAT activation is associated with increased BAT blood flow.[22,30,34] In line with this, we found a trend for a correlation between lower serum tryptophan levels and higher BAT blood flow in cold, supporting hepatic TPO activation as being dependent on BAT activation as well. However, we cannot exclude the possibility that tryptophan utilization is altered in BAT upon cold exposure.

Rodent studies demonstrate that BAT tryptophan concentration increases in mice acutely exposed to cold when compared to animals at thermoneutrality.[11,81] During cold, rodent BAT likely uses tryptophan and kynurenine for *de novo* synthesis of acetyl-CoA rather than NAD^+, given that lower acetyl-CoA levels have been reported in cold-induced BAT in rodents.[82] This is in line with our results showing that tryptophan catabolism for the synthesis of acetyl-CoA via the kynurenine pathway is favored at RT in human BAT in comparison to WAT. Based on our findings, tryptophan degradation in BAT appears to be directly linked with the BAT thermogenic mechanism in humans but, owing to the lack of BAT samples acquired from participants upon cold exposure, the cellular fate of tryptophan in BAT remains unclear in cold-stimulated conditions in humans. However, as acute tryptophan treatment significantly increased the expression of *UCP1* without affecting NAD^+ levels in our *in vitro* experiments in human brite adipocytes, tryptophan likely has a link to BAT thermogenic metabolism via the NAD^+-independent mechanism in humans. Overall, the results from our and other studies suggest that tryptophan is likely metabolized via the kynurenine pathway in the liver and BAT during hypermetabolic cold-stress conditions in humans.

An increase in intracellular NAD^+ levels is closely linked to improved metabolic health.[53,72] We observed that measures of metabolic health were related to the cold-induced circulating levels of both kynurenine and tryptophan and with the expression of NAD^+ biosynthesis and consumption genes. The inverse correlations of kynurenine and tryptophan with indicators of metabolic health are not surprising, given that we also observed these metabolites to be lowered by cold exposure only in persons with high-BAT activation. It is important to highlight that BAT activity has been previously related to these parameters.[23,25,32,33,83,84] Additionally, the lower levels of tryptophan and kynurenine found to be associated with cold-activated BAT are likely beneficial, because their use for the synthesis of metabolites (e.g., kynurenine metabolites) at the cellular level may prevent inflammation, oxidative stress, and harmful immune activation.[85] Regarding the correlations found with gene expression in BAT, we observed that higher NAD^+ biosynthesis is associated with lower body adiposity, higher insulin sensitivity, and a more favorable circulating lipid profile. These findings are in agreement with studies showing that supplementation with NAD^+ precursors is beneficial in mice and humans[10,86] and thereby highlight the importance of continuing to study NAD^+ boosters in human BAT as a potential target to enhance BAT activity for metabolic health benefits.

Limitations of the study

In our study, serum was exploited for metabolomics analysis. Serum does not contain the full spectrum of NAD^+ metabolites other than NAM, its degradation products, NA, and tryptophan. Whole-blood analysis would have given additional information on the NAD^+ metabolome.[87] Our study also does not provide NAD^+ concentration data in human BAT biopsy samples, rather only tryptophan because of the utilization of a non-targeted metabolomics approach. In future studies a targeted method to detect NAD^+ from BAT samples is needed. Additionally, our current data provide a snapshot of the metabolic processes rather than the dynamics of NAD^+ biosynthesis and consumption; future studies using advanced fluxomics techniques may reveal the full spectrum of these simultaneous biological processes. The reason for these limitations is that the study was not initially designed to investigate NAD^+ metabolites but rather the metabolism of BAT by PET-CT imaging and thereby, the model proposed in Figure 7 also possesses inherent limitations; hence, further investigations are needed for robust validation of the model. For ethical reasons, AT samples were not excised during cold stimulation. Therefore, the effect of cold stimulation on the expression of the genes and proteins was not investigated. Nevertheless, paired gene expression between BAT and WAT can indicate the upregulated molecular mechanisms in either AT depot. However, from a different perspective, it is more meaningful to study the expression of these genes at RT because modern-day humans spend most of their time at RT. In addition, clinical interventions with NAD^+ precursor supplementation focus on studying NAD^+ precursor metabolizing enzymes at RT. One additional limitation is that we have evaluated the expression of genes responsible for encoding proteins. Gene mRNA expression levels do not always represent the levels of protein or enzymatic activity, which is a limitation inherent to all

studies employing RNA-sequencing analysis. However, some of the NAD$^+$ biosynthetic enzymes such as NAMPT are only regulated at the level of transcription.[45,88]

Despite these limitations, our study provides intensive insights into the NAD$^+$ precursors NAM and tryptophan in response to cold stimulation in relation to BAT metabolism in adult humans. Because several molecular pathways are distinctly regulated in human BAT in comparison to rodents and these differences remain untangled by the scientific community,[89] our study offers understanding of NAD$^+$ metabolism in BAT in comparison to WAT in adult humans. In addition, our study provides supporting evidence that the regulation of NAD$^+$ metabolism by liver and BAT occurs in a coordinated fashion in cold. It provides a framework for designing and interpreting results from clinical intervention studies seeking to target NAD$^+$ regulation in human BAT for therapeutic purposes.

Conclusions

The present study shows that exposure to cold in adult humans induces changes in serum levels of the NAD$^+$ precursor metabolites NAM, tryptophan, and kynurenine, which are associated with BAT activation during cold exposure. This phenomenon is more profound in the subjects with higher cold-stimulated BAT activity, as assessed by PET imaging. In BAT as compared to WAT, mRNA expression of several genes encoding proteins involved in the biosynthesis of NAD$^+$ is upregulated. In BAT, NAD$^+$ biosynthesis via the salvage pathway enzyme, NAMPT, is likely to be the preferred NAD$^+$ biosynthetic route in cold. The inter-individual variance in the expression of genes involved in cellular NAD$^+$ biosynthesis in BAT and in serum metabolites participating in *de novo* NAD$^+$ biosynthesis is related to systemic metabolic health as assessed by circulatory lipid concentrations and whole-body insulin sensitivity. In human brite adipocytes, acute treatment with NAM or tryptophan is linked to the upregulation of the thermogenic gene *UCP1*. Together, these results reinforce the importance of NAD$^+$ biosynthesis in BAT as a potential target to support BAT activity for metabolic health benefits.

STAR★METHODS

Detailed methods are provided in the online version of this paper and include the following:

SUPPLEMENTAL INFORMATION

Supplemental information can be found online at https://doi.org/10.1016/j.celrep.2023.113131.

ACKNOWLEDGMENTS

The authors thank the staff of the Turku PET Center for their technical assistance and Dr. A.G. Borkowska for project coordination at UC Davis. The study was financially supported by Academy of Finland (grant numbers 259926, 265204, 269977, 272376, 292839, 314383, 314455, 314456, 321716, 335446, 335443, 335445, profi6 336449, 356733, 404030), the Paulo Foundation, the Finnish Cultural Foundation Southwest Finland Regional and Central Funds, the Turku University Hospital Research Funds, the European Union (EUFP7 project 278373; DIABAT) and a joint French/German grant ANR/DFG (Nutribrite), the Finnish Medical Foundation, Gyllenberg Foundation, Novo Nordisk Foundation (grant numbers NNF20OC0060547, NNF17OC0027232, NNF10OC1013354), the Finnish Diabetes Research Foundation, University of Helsinki and Helsinki University Hospital, Government Research Funds, Finnish-Norwegian Medical Research Foundation, Juhani Aho Foundation for Medical Research, Jalmari ja Rauha Ahokkaan Säätiö, Suorsa Foundation, the NIH West Coast Metabolomics Center 5U24DK097154-04, and USDA CRIS Projects 2032-51530-022-00D and 2032-51530-025-00D (J.W.N.). T.F. and M.K. are funded by the German Research Foundation (BATenergy TRR333/1, Deutsche Forschungsgemeinschaft). N.G. and E.-Z.A. are funded by CNRS, Inserm, and UCA. The USDA is an equal opportunity employer and provider. The study was conducted within the Finnish Center of Excellence in Cardiovascular and Metabolic Diseases supported by the Academy of Finland, University of Turku, Turku University Hospital, and Abo Akademi University.

AUTHOR CONTRIBUTIONS

M.U.-D., V.D.d.M., and M.T. drafted the manuscript. M.T., M.L., A.K., and V.D.d.M. contributed to acquiring and interpreting the circulatory serum non-targeted metabolomics data and their main statistical analyses. M.U.-D. and V.D.d.M. performed further statistical analyses and provided the interpretation of metabolomics, clinical, and gene expression data. J.R. conducted the clinical PET-CT imaging study visits and acquired the clinical phenotypic and metabolic health data. T.N. performed the biopsy excision of the BAT and WAT tissue samples. T.F. and M.K. conducted the RNA-seq analyses of the tissue samples. K.K. and J.W.N. performed the tissue metabolomics analyses. K.H., N.G., and E.-Z.A. performed the *in vitro* experimentation, and E.P. analyzed the data. Contributions of K.H.P., J.P., and E.P. were crucial for enhancing the intellectual scientific content of the manuscript, E.P. in particular providing in-depth expertise of NAD$^+$ metabolism. P.N. and K.A.V. contributed to the conception and design of the PET studies and, in addition to K.A.V., K.H. contributed to the conception and design of the circulatory metabolomics study. All authors provided their scientific expertise to critically evaluate the manuscript. E.P., K.H., and K.A.V. were responsible for revising and approving the final edition of the manuscript.

DECLARATION OF INTERESTS

The authors declare no competing interests.

INCLUSION AND DIVERSITY

We support inclusive, diverse, and equitable conduct of research.

Received: May 31, 2022
Revised: July 6, 2023
Accepted: August 29, 2023
Published: September 13, 2023

REFERENCES

1. Schrauwen, P., and van Marken Lichtenbelt, W.D. (2016). Combatting type 2 diabetes by turning up the heat. Diabetologia *59*, 2269–2279.
2. Saito, M., Okamatsu-Ogura, Y., Matsushita, M., Watanabe, K., Yoneshiro, T., Nio-Kobayashi, J., Iwanaga, T., Miyagawa, M., Kameya, T., Nakada, K., et al. (2009). High Incidence of Metabolically Active Brown Adipose Tissue in Healthy Adult Humans: Effects of Cold Exposure and Adiposity. Diabetes *58*. 1526–31.
3. Lee, P., Smith, S., Linderman, J., Courville, A.B., Brychta, R.J., Dieckmann, W., Werner, C.D., Chen, K.Y., and Celi, F.S. (2014). Temperature-acclimated brown adipose tissue modulates insulin sensitivity in humans. Diabetes *63*, 3686–3698.
4. Scheele, C., and Nielsen, S. (2017). Metabolic regulation and the anti-obesity perspectives of human brown fat. Redox Biol. *12*, 770–775. https://pubmed.ncbi.nlm.nih.gov/28431377/.
5. Schlein, C., and Heeren, J. (2016). Implications of thermogenic adipose tissues for metabolic health. Best Pract. Res. Clin. Endocrinol. Metab. *30*, 487–496. https://pubmed.ncbi.nlm.nih.gov/27697210/.
6. Nedergaard, J., Golozoubova, V., Matthias, A., Asadi, A., Jacobsson, A., and Cannon, B. (2001). UCP1: The Only Protein Able to Mediate Adaptive Non-shivering Thermogenesis and Metabolic Inefficiency, *1504* (Biochimica et Biophysica Acta - Bioenergetics), pp. 82–106.
7. Hanssen, M.J.W., Van Der Lans, A.A.J.J., Brans, B., Hoeks, J., Jardon, K.M.C., Schaart, G., Mottaghy, F.M., Schrauwen, P., and Van Marken Lichtenbelt, W.D. (2016). Short-term cold acclimation recruits brown adipose tissue in obese humans. Diabetes *65*, 1179–1189.
8. Hanssen, M.J.W., Hoeks, J., Brans, B., van der Lans, A.A.J.J., Schaart, G., van den Driessche, J.J., Jörgensen, J.A., Boekschoten, M.V., Hesselink, M.K.C., Havekes, B., et al. (2015). Short-term cold acclimation improves insulin sensitivity in patients with type 2 diabetes mellitus. Nat. Med. *21*, 863–865. https://doi.org/10.1038/nm.3891.
9. O'Mara, A.E., Johnson, J.W., Linderman, J.D., Brychta, R.J., McGehee, S., Fletcher, L.A., Fink, Y.A., Kapuria, D., Cassimatis, T.M., Kelsey, N., et al. (2020). Chronic mirabegron treatment increases human brown fat, HDL cholesterol, and insulin sensitivity. J. Clin. Invest. *130*, 2209–2219. https://pubmed.ncbi.nlm.nih.gov/31961826/.
10. Cantó, C., Menzies, K.J., and Auwerx, J. (2015). NAD+ Metabolism and the Control of Energy Homeostasis: A Balancing Act between Mitochondria and the Nucleus. Cell Metabolism *22*, 31–53. Cell Press.
11. Yamaguchi, S., Franczyk, M.P., Chondronikola, M., Qi, N., Gunawardana, S.C., Stromsdorfer, K.L., Porter, L.C., Wozniak, D.F., Sasaki, Y., Rensing, N., et al. (2019). Adipose tissue NAD+ biosynthesis is required for regulating adaptive thermogenesis and whole-body energy homeostasis in mice. Proc. Natl. Acad. Sci. USA *116*, 23822–23828. https://www.pnas.org/content/116/47/23822.
12. Pan, X.R., Li, G.W., Hu, Y.H., Wang, J.X., Yang, W.Y., An, Z.X., Hu, Z.X., Lin, J., Xiao, J.Z., Cao, H.B., et al. (1997). Effects of diet and exercise in preventing NIDDM in people with impaired glucose tolerance. The Da Qing IGT and Diabetes Study. Diabetes Care *20*, 537–544. https://pubmed.ncbi.nlm.nih.gov/9096977/.
13. Yoshino, J., Mills, K.F., Yoon, M.J., and Imai, S.I. (2011). Nicotinamide mononucleotide, a key NAD(+) intermediate, treats the pathophysiology of diet- and age-induced diabetes in mice. Cell Metab. *14*, 528–536. https://pubmed.ncbi.nlm.nih.gov/21982712/.
14. Katsyuba, E., Mottis, A., Zietak, M., De Franco, F., van der Velpen, V., Gariani, K., Ryu, D., Cialabrini, L., Matilainen, O., Liscio, P., et al. (2018). De novo NAD+ synthesis enhances mitochondrial function and improves health. Nature *563*, 354–359. https://pubmed.ncbi.nlm.nih.gov/30356218/.
15. Lee, H.J., Hong, Y.S., Jun, W., and Yang, S.J. (2015). Nicotinamide Riboside Ameliorates Hepatic Metaflammation by Modulating NLRP3 Inflammasome in a Rodent Model of Type 2 Diabetes. J. Med. Food *18*, 1207–1213. https://pubmed.ncbi.nlm.nih.gov/25974041/.
16. Pirinen, E., Auranen, M., Khan, N.A., Brilhante, V., Urho, N., Pessia, A., Hakkarainen, A., Kuula, J., Heinonen, U., Schmidt, M.S., et al. (2020). Niacin Cures Systemic NAD+ Deficiency and Improves Muscle Performance in Adult-Onset Mitochondrial Myopathy. Cell Metab. *31*, 1078–1090.e5. https://pubmed.ncbi.nlm.nih.gov/32386566/.
17. Bai, P., Canto, C., Brunyánszki, A., Huber, A., Szántó, M., Cen, Y., Yamamoto, H., Houten, S.M., Kiss, B., Oudart, H., et al. (2011). PARP-2 regulates SIRT1 expression and whole-body energy expenditure. Cell Metab. *13*, 450–460. https://pubmed.ncbi.nlm.nih.gov/21459329/.
18. Bai, P., Cantó, C., Oudart, H., Brunyánszki, A., Cen, Y., Thomas, C., Yamamoto, H., Huber, A., Kiss, B., Houtkooper, R.H., et al. (2011). PARP-1 inhibition increases mitochondrial metabolism through SIRT1 activation. Cell Metab. *13*, 461–468.
19. Benzi, A., Sturla, L., Heine, M., Fischer, A.W., Spinelli, S., Magnone, M., Sociali, G., Parodi, A., Fenoglio, D., Emionite, L., et al. (2021). CD38 downregulation modulates NAD+ and NADP(H) levels in thermogenic adipose tissues. Biochim. Biophys. Acta. Mol. Cell Biol. Lipids *1866*, 158819. https://pubmed.ncbi.nlm.nih.gov/33010451/.
20. Khan, N.A., Auranen, M., Paetau, I., Pirinen, E., Euro, L., Forsström, S., Pasila, L., Velagapudi, V., Carroll, C.J., Auwerx, J., and Suomalainen, A. (2014). Effective treatment of mitochondrial myopathy by nicotinamide riboside, a vitamin B3. EMBO Mol. Med. *6*, 721–731. https://pubmed.ncbi.nlm.nih.gov/24711540/.
21. Nascimento, E.B.M., Moonen, M.P.B., Remie, C.M.E., Gariani, K., Jörgensen, J.A., Schaart, G., Hoeks, J., Auwerx, J., van Marken Lichtenbelt, W.D., and Schrauwen, P. (2021). Nicotinamide Riboside Enhances In Vitro Beta-adrenergic Brown Adipose Tissue Activity in Humans. J. Clin. Endocrinol. Metab. *106*, 1437–1447. https://academic.oup.com/jcem/article/106/5/1437/6125711.
22. Orava, J., Nuutila, P., Lidell, M.E., Oikonen, V., Noponen, T., Viljanen, T., Scheinin, M., Taittonen, M., Niemi, T., Enerbäck, S., and Virtanen, K.A. (2011). Different metabolic responses of human brown adipose tissue to activation by cold and insulin. Cell Metab. *14*, 272–279.
23. U Din, M., Raiko, J., Saari, T., Saunavaara, V., Kudomi, N., Solin, O., Parkkola, R., Nuutila, P., and Virtanen, K.A. (2017). Human brown fat radiodensity indicates underlying tissue composition and systemic metabolic health. J. Clin. Endocrinol. Metab. *102*, 2258–2267.
24. U Din, M., Saari, T., Raiko, J., Kudomi, N., Maurer, S.F., Lahesmaa, M., Fromme, T., Amri, E.Z., Klingenspor, M., Solin, O., et al. (2018). Postprandial Oxidative Metabolism of Human Brown Fat Indicates Thermogenesis. Cell Metab. http://www.ncbi.nlm.nih.gov/pubmed/29909972
25. Saari, T.J., Raiko, J., U-Din, M., Niemi, T., Taittonen, M., Laine, J., Savisto, N., Haaparanta-Solin, M., Nuutila, P., and Virtanen, K.A. (2020). Basal and cold-induced fatty acid uptake of human brown adipose tissue is impaired in obesity. Sci. Rep. *10*, 14373. https://doi.org/10.1038/s41598-020-71197-2.
26. Simcox, J., Geoghegan, G., Maschek, J.A., Bensard, C.L., Pasquali, M., Miao, R., Lee, S., Jiang, L., Huck, I., Kershaw, E.E., et al. (2017). Global analysis of plasma lipids identifies liver-derived acylcarnitines as a fuel source for brown fat thermogenesis. Cell Metab. *26*, 509–522.e6.
27. Chondronikola, M., Volpi, E., Børsheim, E., Porter, C., Saraf, M.K., Annamalai, P., Yfanti, C., Chao, T., Wong, D., Shinoda, K., et al. (2016). Brown Adipose Tissue Activation Is Linked to Distinct Systemic Effects on Lipid Metabolism in Humans. Cell Metab. *23*, 1200–1206.
28. Baba, S., Jacene, H.A., Engles, J.M., Honda, H., and Wahl, R.L. (2010). CT Hounsfield Units of Brown Adipose Tissue Increase with Activation: Preclinical and Clinical Studies. J. Nucl. Med. *51*, 246–250. http://jnm.snmjournals.org/cgi/doi/10.2967/jnumed.109.068775.

29. Muzik, O., Mangner, T.J., and Granneman, J.G. (2012). Assessment of Oxidative Metabolism in Brown Fat Using PET Imaging. Front Endocrinol.(Lausanne) *3*, 15.

30. Muzik, O., Mangner, T.J., Leonard, W.R., Kumar, A., Janisse, J., and Granneman, J.G. (2013). 15O PET Measurement of Blood Flow and Oxygen Consumption in Cold-Activated Human Brown Fat [Internet]. J. Nucl. Med. *54*, 523–531. https://doi.org/10.2967/jnumed.112.111336.

31. Ernande, L., Stanford, K.I., Thoonen, R., Zhang, H., Clerte, M., Hirshman, M.F., Goodyear, L.J., Bloch, K.D., Buys, E.S., and Scherrer-Crosbie, M. (2016). Relationship of brown adipose tissue perfusion and function: a study through β2-adrenoreceptor stimulation. J. Appl. Physiol. *120*, 825–832. https://doi.org/10.1152/japplphysiol.00634.2015.

32. Motiani, P., Virtanen, K.A., Motiani, K.K., Eskelinen, J.J., Middelbeek, R.J., Goodyear, L.J., Savolainen, A.M., Kemppainen, J., Jensen, J., Din, M.U., et al. (2017). Decreased insulin-stimulated brown adipose tissue glucose uptake after short-term exercise training in healthy middle aged men. Diabetes Obes. Metab. http://www.ncbi.nlm.nih.gov/pubmed/28318098

33. Raiko, J., Orava, J., Savisto, N., and Virtanen, K.A. (2020). High Brown Fat Activity Correlates With Cardiovascular Risk Factor Levels Cross-Sectionally and Subclinical Atherosclerosis at 5-Year Follow-Up. Arterioscler. Thromb. Vasc. Biol. *40*, 1289–1295. https://pubmed.ncbi.nlm.nih.gov/31941384/.

34. U Din, M., Raiko, J., Saari, T., Kudomi, N., Tolvanen, T., Oikonen, V., Teuho, J., Sipilä, H.T., Savisto, N., Parkkola, R., et al. (2016). Human brown adipose tissue [15O]O2 PET imaging in the presence and absence of cold stimulus. Eur. J. Nucl. Med. Mol. Imaging *43*, 1878–1886.

35. Ratajczak, J., Joffraud, M., Trammell, S.A.J., Ras, R., Canela, N., Boutant, M., Kulkarni, S.S., Rodrigues, M., Redpath, P., Migaud, M.E., et al. (2016). NRK1 controls nicotinamide mononucleotide and nicotinamide riboside metabolism in mammalian cells. Nat. Commun. *7*, 13103. https://pubmed.ncbi.nlm.nih.gov/27725675/.

36. Liu, L., Su, X., Quinn, W.J., Hui, S., Krukenberg, K., Frederick, D.W., Redpath, P., Zhan, L., Chellappa, K., White, E., et al. (2018). Quantitative Analysis of NAD Synthesis-Breakdown Fluxes. Cell Metab. *27*, 1067–1080.e5. http://www.cell.com/article/S1550413118301967/fulltext.

37. Denu, J.M. (2007). Vitamins and Aging: Pathways to NAD+ Synthesis. Cell. Cell *129*. https://pubmed.ncbi.nlm.nih.gov/17482537/. 453–4.

38. Bogan, K.L., and Brenner, C. (2008). Nicotinic acid, nicotinamide, and nicotinamide riboside: A molecular evaluation of NAD+ precursor vitamins in human nutrition. Annu. Rev. Nutr. *28*. https://pubmed.ncbi.nlm.nih.gov/18429699/. 115–30.

39. KEGG Pathway Database (2023). KEGG PATHWAY: Nicotinate and Nicotinamide Metabolism - Homo sapiens. (human) [Internet]. 2023 [cited 2023 Jul 31]. https://www.genome.jp/pathway/hsa00760.

40. KEGG Pathway Database (2023). KEGG PATHWAY: Tryptophan Metabolism - Homo sapiens. (human) [Internet]. 2023 [cited 2023 Jul 31]. https://www.genome.jp/kegg-bin/show_pathway?hsa00380.

41. Matthias, A., Ohlson, K.B., Fredriksson, J.M., Jacobsson, A., Nedergaard, J., and Cannon, B. (2000). Thermogenic responses in brown fat cells are fully UCP1-dependent. UCP2 or UCP3 do not substitute for UCP1 in adrenergically or fatty scid-induced thermogenesis. J. Biol. Chem. *275*, 25073–25081. https://pubmed.ncbi.nlm.nih.gov/10825155/.

42. Hornyák, L., Dobos, N., Koncz, G., Karányi, Z., Páll, D., Szabó, Z., Halmos, G., and Székvölgyi, L. (2018). The role of indoleamine-2,3-dioxygenase in cancer development, diagnostics, and therapy. Front. Immunol. *9*, 31. https://www.proteinatlas.org/ENSG00000131203-IDO1/tissue.

43. Krebs, H.A. (1948). The tricarboxylic acid cycle. Harvey Lect. *Series 44*, 165–199. http://www.ncbi.nlm.nih.gov/pubmed/14849928.

44. Verdin, E. (2015). NAD+ in Aging, Metabolism, and Neurodegeneration. Science *350*, 1208–1213. https://pubmed.ncbi.nlm.nih.gov/26785480/.

45. Revollo, J.R., Grimm, A.A., and Imai, S.I. (2007). The regulation of nicotinamide adenine dinucleotide biosynthesis by Nampt/PBEF/visfatin in mammals. Curr. Opin. Gastroenterol. *23*, 164–170. https://pubmed.ncbi.nlm.nih.gov/17268245/.

46. Houtkooper, R.H., Pirinen, E., and Auwerx, J. (2012). Sirtuins as regulators of metabolism and healthspan. Nat. Rev. Mol. Cell Biol. *13*, 225–238. https://www.nature.com/articles/nrm3293.

47. Sebaa, R., Johnson, J., Pileggi, C., Norgren, M., Xuan, J., Sai, Y., Tong, Q., Krystkowiak, I., Bondy-Chorney, E., Davey, N.E., et al. (2019). SIRT3 controls brown fat thermogenesis by deacetylation regulation of pathways upstream of UCP1. Mol. Metab. *25*, 35–49. https://pubmed.ncbi.nlm.nih.gov/31060926/.

48. Lombard, D.B., Alt, F.W., Cheng, H.L., Bunkenborg, J., Streeper, R.S., Mostoslavsky, R., Kim, J., Yancopoulos, G., Valenzuela, D., Murphy, A., et al. (2007). Mammalian Sir2 homolog SIRT3 regulates global mitochondrial lysine acetylation. Mol. Cell Biol. *27*, 8807–8814. https://pubmed.ncbi.nlm.nih.gov/17923681/.

49. Porter, L.C., Franczyk, M.P., Pietka, T., Yamaguchi, S., Lin, J.B., Sasaki, Y., Verdin, E., Apte, R.S., and Yoshino, J. (2018). NAD+-dependent deacetylase SIRT3 in adipocytes is dispensable for maintaining normal adipose tissue mitochondrial function and whole body metabolism. Am. J. Physiol. Endocrinol. Metab. *315*, E520–E530.

50. Wang, G., Meyer, J.G., Cai, W., Li, M.E., Softic, S., and Kahn, C.R. (2018). Sirt5 Plays a Critical Role in Mitochondrial Protein Acylation and Mitochondrial Metabolic Homeostasis in Brown Fat. Diabetes *67*.

51. Laurent, G., German, N.J., Saha, A.K., de Boer, V.C.J., Davies, M., Koves, T.R., Dephoure, N., Fischer, F., Boanca, G., Vaitheesvaran, B., et al. (2013). SIRT4 Coordinates the Balance between Lipid Synthesis and Catabolism by Repressing Malonyl CoA Decarboxylase. Mol. Cell *50*, 686–698.

52. Grozio, A., Mills, K.F., Yoshino, J., Bruzzone, S., Sociali, G., Tokizane, K., Lei, H.C., Cunningham, R., Sasaki, Y., Migaud, M.E., and Imai, S.I. (2019). Slc12a8 is a nicotinamide mononucleotide transporter. Nat. Metab. *1*, 47–57. https://pubmed.ncbi.nlm.nih.gov/31131364/.

53. Chini, C.C.S., Zeidler, J.D., Kashyap, S., Warner, G., and Chini, E.N. (2021). Evolving concepts in NAD+ metabolism. Cell Metab. *33*, 1076–1087. https://pubmed.ncbi.nlm.nih.gov/33930322/.

54. Bhutia, Y.D., Babu, E., and Ganapathy, V. (2015). Interferon-γ induces a tryptophan-selective amino acid transporter in human colonic epithelial cells and mouse dendritic cells. Biochim. Biophys. Acta *1848*, 453–462. https://pubmed.ncbi.nlm.nih.gov/25450809/.

55. Thwaites, D.T., and Anderson, C.M.H. (2011). The SLC36 family of proton-coupled amino acid transporters and their potential role in drug transport. British Journal of Pharmacology, *164* (Br J Pharmacol). https://pubmed.ncbi.nlm.nih.gov/21501141/. 1802–16.

56. Nałęcz, K.A. (2020). Amino Acid Transporter SLC6A14 (ATB0,+) – A Target in Combined Anti-cancer Therapy [Internet]. Front. Cell Dev. Biol. *8*, 1178. www.frontiersin.org.

57. Jiang, Y., Rose, A.J., Sijmonsma, T.P., Bröer, A., Pfenninger, A., Herzig, S., Schmoll, D., and Bröer, S. (2015). Mice lacking neutral amino acid transporter B0AT1 (Slc6a19) have elevated levels of FGF21 and GLP-1 and improved glycaemic control. Mol. Metab. *4*, 406–417.

58. Gopal, E., Fei, Y.J., Miyauchi, S., Zhuang, L., Prasad, P.D., and Ganapathy, V. (2005). Sodium-coupled and electrogenic transport of B-complex vitamin nicotinic acid by slc5a8, a member of the Na/glucose co-transporter gene family. Biochem. J. *388*, 309–316.

59. Bahn, A., Hagos, Y., Reuter, S., Balen, D., Brzica, H., Krick, W., Burckhardt, B.C., Sabolić, I., and Burckhardt, G. (2008). Identification of a new urate and high affinity nicotinate transporter, hOAT10 (SLC22A13). J. Biol. Chem. *283*, 16332–16341. https://pubmed.ncbi.nlm.nih.gov/18411268/.

60. Schuette, S.A., and Rose, R.C. (1983). Nicotinamide uptake and metabolism by chick intestine. Am. J. Physiol. Gastrointest. Liver Physiol. *8*. https://pubmed.ncbi.nlm.nih.gov/6226205/.

61. Sofue, M., Yoshimura, Y., Nishida, M., and Kawada, J. (1991). Uptake of nicotinamide by rat pancreatic β cells with regard to streptozotocin action. J. Endocrinol. *131*, 135–138. https://pubmed.ncbi.nlm.nih.gov/1836006/.

62. Kory, N., uit de Bos, J., van der Rijt, S., Jankovic, N., Güra, M., Arp, N., Pena, I.A., Prakash, G., Chan, S.H., Kunchok, T., et al. (2020). MCART1/SLC25A51 is required for mitochondrial NAD transport. Sci. Adv. *6*, eabe5310. http://advances.sciencemag.org/.

63. Luongo, T.S., Eller, J.M., Lu, M.J., Niere, M., Raith, F., Perry, C., Bornstein, M.R., Oliphint, P., Wang, L., McReynolds, M.R., et al. (2020). SLC25A51 is a mammalian mitochondrial NAD+ transporter. Nature *1–6*. https://www.nature.com/articles/s41586-020-2741-7.

64. Davila, A., Liu, L., Chellappa, K., Redpath, P., Nakamaru-Ogiso, E., Paolella, L.M., Zhang, Z., Migaud, M.E., Rabinowitz, J.D., and Baur, J.A. (2018). Nicotinamide adenine dinucleotide is transported into mammalian mitochondria. Elife *7*, e33246. https://pubmed.ncbi.nlm.nih.gov/29893687/.

65. Formentini, L., Moroni, F., and Chiarugi, A. (2009). Detection and pharmacological modulation of nicotinamide mononucleotide (NMN) in vitro and in vivo. Biochem. Pharmacol. *77*, 1612–1620. https://pubmed.ncbi.nlm.nih.gov/19426698/.

66. Jokinen, R., Pirnes-Karhu, S., Pietiläinen, K.H., and Pirinen, E. (2017). Adipose tissue NAD+-homeostasis, sirtuins and poly(ADP-ribose) polymerases -important players in mitochondrial metabolism and metabolic health. Redox Biol. *12*, 246–263. https://pubmed.ncbi.nlm.nih.gov/28279944/.

67. Xie, N., Zhang, L., Gao, W., Huang, C., Huber, P.E., Zhou, X., Li, C., Shen, G., and Zou, B. (2020). NAD+ metabolism: pathophysiologic mechanisms and therapeutic potential. Signal Transduct. Target. Ther. *5*, 227–237. https://www.nature.com/articles/s41392-020-00311-7.

68. Aksoy, S., Szumlanski, C.L., and Weinshilboum, R.M. (1994). Human liver nicotinamide N-methyltransferase. cDNA cloning, expression, and biochemical characterization. J. Biol. Chem. *269*, 14835–14840. https://europepmc.org/article/MED/8182091.

69. Felsted, R.L., and Chaykin, S. (1967). N1-Methylnicotinamide Oxidation in a Number of Mammals. J. Biol. Chem. *242*, 1274–1279.

70. Sarett, H.P., and Goldsmith, G.A. (1949). Tryptophan and nicotinic acid studies in man. J. Biol. Chem. *177*, 461–475.

71. Imai, S.I., and Guarente, L. (2016). It takes two to tango: NAD+ and sirtuins in aging/longevity control. NPJ Aging Mech. Dis. *2*, 16017.

72. Katsyuba, E., Romani, M., Hofer, D., and Auwerx, J. (2020). NAD+ homeostasis in health and disease. Nat. Metab. *2*, 9–31. https://pubmed.ncbi.nlm.nih.gov/32694684/.

73. Crisol, B.M., Veiga, C.B., Lenhare, L., Braga, R.R., Silva, V.R.R., da Silva, A.S.R., Cintra, D.E., Moura, L.P., Pauli, J.R., and Ropelle, E.R. (2018). Nicotinamide riboside induces a thermogenic response in lean mice. Life Sci. *211*, 1–7. https://pubmed.ncbi.nlm.nih.gov/30195617/.

74. Méndez-Lara, K.A., Rodríguez-Millán, E., Sebastián, D., Blanco-Soto, R., Camacho, M., Nan, M.N., Diarte-Añazco, E.M.G., Mato, E., Lope-Piedrafita, S., Roglans, N., et al. (2021). Nicotinamide Protects Against Diet-Induced Body Weight Gain, Increases Energy Expenditure, and Induces White Adipose Tissue Beiging. Mol. Nutr. Food Res. *65*, e2100111. https://pubmed.ncbi.nlm.nih.gov/33870623/.

75. Badawy, A.A.B. (2017). Kynurenine Pathway of Tryptophan Metabolism: Regulatory and Functional Aspects. Int. J. Tryptophan Res. *10*, 1178646917691938. https://pubmed.ncbi.nlm.nih.gov/28469468/.

76. Fukuwatari, T., and Shibata, K. (2013). Nutritional aspect of tryptophan metabolism. Int. J. Tryptophan Res. *6* (*Suppl 1*), 3–8. https://pubmed.ncbi.nlm.nih.gov/23922498/.

77. Richard, D.M., Dawes, M.A., Mathias, C.W., Acheson, A., Hill-Kapturczak, N., and Dougherty, D.M. (2009). L-Tryptophan: Basic Metabolic Functions, Behavioral Research and Therapeutic Indications. Int. J. Tryptophan Res. *2*, 45–60. https://pubmed.ncbi.nlm.nih.gov/20651948/.

78. Sitaramam, V., and Ramasarma, T. (1975). Nature of induction of tryptophan pyrrolase in cold exposure. J. Appl. Physiol. *38*, 245–249. https://pubmed.ncbi.nlm.nih.gov/1120747/.

79. KNOX, W.E. (1951). Two Mechanisms which Increase in vivo the Liver Tryptophan Peroxidase Activity: Specific Enzyme Adaptation and Stimulation of the Pituitary-Adrenal System. Br. J. Exp. Pathol. *32*, 462–469. https://www.ncbi.nlm.nih.gov/pmc/articles/PMC2073205/.

80. Alba, B.K., Castellani, J.W., and Charkoudian, N. (2019). Cold-induced cutaneous vasoconstriction in humans: Function, dysfunction and the distinctly counterproductive. Exp. Physiol. *104*, 1202–1214. https://pubmed.ncbi.nlm.nih.gov/31045297/.

81. Okamatsu-Ogura, Y., Kuroda, M., Tsutsumi, R., Tsubota, A., Saito, M., Kimura, K., and Sakaue, H. (2020). UCP1-dependent and UCP1-independent metabolic changes induced by acute cold exposure in brown adipose tissue of mice. Metabolism *113*, 154396. https://pubmed.ncbi.nlm.nih.gov/33065161/.

82. Hiroshima, Y., Yamamoto, T., Watanabe, M., Baba, Y., and Shinohara, Y. (2018). Effects of cold exposure on metabolites in brown adipose tissue of rats. Mol. Genet. Metab. Rep. *15*, 36–42. https://pubmed.ncbi.nlm.nih.gov/30023288/.

83. Matsushita, M., Yoneshiro, T., Aita, S., Kameya, T., Sugie, H., and Saito, M. (2014). Impact of brown adipose tissue on body fatness and glucose metabolism in healthy humans. Int. J. Obes. *38*, 812–817. http://www.ncbi.nlm.nih.gov/pubmed/24213309.

84. Becher, T., Palanisamy, S., Kramer, D.J., Eljalby, M., Marx, S.J., Wibmer, A.G., Butler, S.D., Jiang, C.S., Vaughan, R., Schöder, H., et al. (2021). Brown adipose tissue is associated with cardiometabolic health. Nat. Med. *27*, 58–65. https://www.nature.com/articles/s41591-020-1126-7.

85. Groth, B., Venkatakrishnan, P., and Lin, S.J. (2021). NAD+ Metabolism, Metabolic Stress, and Infection. Front. Mol. Biosci. *8*, 686412. https://pubmed.ncbi.nlm.nih.gov/34095234/.

86. Lapatto, H.A.K., Kuusela, M., Heikkinen, A., Muniandy, M., van der Kolk, B.W., Gopalakrishnan, S., Pöllänen, N., Sandvik, M., Schmidt, M.S., Heinonen, S., et al. (2023). Nicotinamide riboside improves muscle mitochondrial biogenesis, satellite cell differentiation, and gut microbiota in a twin study. Sci. Adv. *9*, eadd5163. https://pubmed.ncbi.nlm.nih.gov/36638183/.

87. Trammell, S.A.J., Schmidt, M.S., Weidemann, B.J., Redpath, P., Jaksch, F., Dellinger, R.W., Li, Z., Abel, E.D., Migaud, M.E., and Brenner, C. (2016). Nicotinamide riboside is uniquely and orally bioavailable in mice and humans. Nat. Commun. *7*, 12948.

88. Revollo, J.R., Körner, A., Mills, K.F., Satoh, A., Wang, T., Garten, A., Dasgupta, B., Sasaki, Y., Wolberger, C., Townsend, R.R., et al. (2007). Nampt/PBEF/Visfatin regulates insulin secretion in beta cells as a systemic NAD biosynthetic enzyme. Cell Metab. *6*, 363–375. https://pubmed.ncbi.nlm.nih.gov/17983582/.

89. Liu, X., Cervantes, C., and Liu, F. (2017). Common and Distinct Regulation of Human and Mouse Brown and Beige Adipose Tissues: A Promising Therapeutic Target for Obesity. Protein Cell *8*. 446–54.

90. Rodriguez, A.M., Pisani, D., Dechesne, C.A., Turc-Carel, C., Kurzenne, J.Y., Wdziekonski, B., Villageois, A., Bagnis, C., Breittmayer, J.P., Groux, H., et al. (2005). Transplantation of a multipotent cell population from human adipose tissue induces dystrophin expression in the immunocompetent mdx mouse. J. Exp. Med. *201*, 1397–1405. https://pubmed.ncbi.nlm.nih.gov/15867092/.

91. Bates, D.W., Mächler, M., Bolker, B.M., and Walker, S.C. (2015). Fitting Linear Mixed-Effects Models Using lme4. BMJ Qual. Saf. *24*, 1–3. https://www.jstatsoft.org/index.php/jss/article/view/v067i01.

92. Chen, K.Y., Cypess, A.M., Laughlin, M.R., Haft, C.R., Hu, H.H., Bredella, M.A., Enerbäck, S., Kinahan, P.E., Lichtenbelt, W.v.M., Lin, F.I., et al. (2016). Brown Adipose Reporting Criteria in Imaging STudies (BARCIST 1.0): Recommendations for Standardized FDG-PET/CT Experiments in Humans. Cell Metab. *24*, 210–222. https://pubmed.ncbi.nlm.nih.gov/27508870/.

93. Friedewald, W.T., Levy, R.I., and Fredrickson, D.S. (1972). Estimation of the concentration of low-density lipoprotein cholesterol in plasma, without use of the preparative ultracentrifuge. Clin. Chem. *18*, 499–502. http://www.ncbi.nlm.nih.gov/pubmed/4337382.

94. Elabd, C., Chiellini, C., Carmona, M., Galitzky, J., Cochet, O., Petersen, R., Pénicaud, L., Kristiansen, K., Bouloumié, A., Casteilla, L., et al. (2009). Human multipotent adipose-derived stem cells differentiate into functional brown adipocytes. Stem Cell. *27*, 2753–2760. https://pubmed.ncbi.nlm.nih.gov/19697348/.

95. Pisani, D.F., Djedaini, M., Beranger, G.E., Elabd, C., Scheideler, M., Ailhaud, G., and Amri, E.Z. (2011). Differentiation of Human Adipose-Derived Stem Cells into "Brite" (Brown-in-White) Adipocytes. Front Endocrinol (Lausanne)*2*. https://pubmed.ncbi.nlm.nih.gov/22654831/.

96. Sumner, L.W., Amberg, A., Barrett, D., Beale, M.H., Beger, R., Daykin, C.A., Fan, T.W.M., Fiehn, O., Goodacre, R., Griffin, J.L., et al. (2007). Proposed minimum reporting standards for chemical analysis Chemical Analysis Working Group (CAWG) Metabolomics Standards Initiative (MSI). Metabolomics *3*, 211–221. https://pubmed.ncbi.nlm.nih.gov/24039616/.

97. Klåvus, A., Kokla, M., Noerman, S., Koistinen, V.M., Tuomainen, M., Zarei, I., Meuronen, T., Häkkinen, M.R., Rummukainen, S., Farizah Babu, A., et al. (2020). Notame": Workflow for Non-Targeted LC–MS Metabolic Profiling. Metab. *10*, 135. https://www.mdpi.com/2218-1989/10/4/135/htm.

98. R Core Team. R: A Language and Environment for Statistical Computing | BibSonomy [Internet]. 2007. [cited 2023 Jul 31]. https://www.bibsonomy.org/bibtex/7469ffee3b07f9167cf47e7555041ee7

99. Broadhurst, D., Goodacre, R., Reinke, S.N., Kuligowski, J., Wilson, I.D., Lewis, M.R., and Dunn, W.B. (2018). Guidelines and considerations for the use of system suitability and quality control samples in mass spectrometry assays applied in untargeted clinical metabolomic studies. Metabolomics *14*, 72. https://pubmed.ncbi.nlm.nih.gov/29805336/.

100. Kirwan, J.A., Broadhurst, D.I., Davidson, R.L., and Viant, M.R. (2013). Characterising and correcting batch variation in an automated direct infusion mass spectrometry (DIMS) metabolomics workflow. Anal. Bioanal. Chem. *405*, 5147–5157. https://doi.org/10.1007/s00216-013-6856-7.

101. Stekhoven, D.J., and Bühlmann, P. (2012). MissForest—non-parametric missing value imputation for mixed-type data. Bioinformatics *28*, 112–118. https://doi.org/10.1093/bioinformatics/btr597.

102. Kuznetsova, A., Brockhoff, P.B., and Christensen, R.H.B. (2017). lmerTest Package: Tests in Linear Mixed Effects Models. J. Stat. Softw. *82*, 1–26. https://www.jstatsoft.org/index.php/jss/article/view/v082i13.

STAR★METHODS

KEY RESOURCES TABLE

REAGENT or RESOURCE	SOURCE	IDENTIFIER
Biological samples		
Human BAT & WAT biopsies	Human BAT Metabolism Research Group, Turku PET Center, Finland https://hbat.utu.fi/	N/A
Human serum samples	Human BAT Metabolism Research Group, Turku PET Center, Finland https://hbat.utu.fi/	N/A
Critical commercial assays		
TruSeq RNA Access Coding Transcriptome	Illumina	Cat# RS-301-2001
Q-NAD Tissue/Cell NAD+ assay kit	NADMED Ltd, Finland	cat no: RUO_003
BCA protein assay kit	Pierce™	cat no: 23227
Deposited data		
RNA-Seq data	Tissue samples from this study	GEO: GSE113764
Serum Non-targeted Metabolomics Data	Serum samples from this study	National Metabolomics Data Repository (NMDR) Study ID: ST002826 https://doi.org/10.21228/M85T5M
Experimental models: Cell lines		
Human Multipotent Adipose-Derived Stem (hMADS) cells	Rodriguez et al.[90]	N/A
Software and algorithms		
Carimas, PET-CT image data analysis software	Turku PET Center	http://turkupetcentre.fi/carimas/
IBM SPSS Statistics 22	IBM	RRID: SCR_002865
GraphPad Prism 9	GraphPad Software	RRID: SCR_002798
MassHunter Acquisition	Agilent Technologies	B.05.01
MS-DIAL software 3.52	RIKEN Center for Sustainable Resource Science	http://prime.psc.riken.jp/Metabolomics_Software/index.html
R programming/R studio	Posit	version 3.5.1
lme4 R package	Bates et al.[91]	version 1.1.20
Other		
[^{15}O]H_2O, radiotracer	Turku PET Center, Hidex Radiowater Generator	http://turkupetcentre.fi/radiochemistry/, http://hidex.com/
[^{18}F]FTHA, radiotracer	Turku PET Center radiochemistry	http://turkupetcentre.fi/radiochemistry/
[^{18}F]FDG, radiotracer	Turku PET Center radiochemistry	http://turkupetcentre.fi/radiochemistry/
Blanketrol III (cooling blanket)	Cincinnati Sub-Zero	https://www.cszmedical.com/blanketrol-iii
Quadrupole time-of-flight mass spectrometry (UHPLC–qTOF-MS) system	Agilent Technologies	N/A

RESOURCE AVAILABILITY

Lead contact

Further information and requests for resources and reagents should be directed to and will be fulfilled by the lead contact. The lead contact is Professor Kirsi A. Virtanen (kirsi.virtanen@utu.fi).

Materials availability

This study did not generate new or unique reagents.

Data and code availability

- RNA-Seq data have been deposited at NCBI's Gene Expression Omnibus (GEO) and are accessible through GEO: GSE113764. Metabolomics data have been deposited at NIH Common Fund's National Metabolomics Data Repository (NMDR) Website, the Metabolomics Workbench, https://www.metabolomicsworkbench.org where it has been assigned Study ID ST002826. The data can be accessed directly via its Project DOI: https://doi.org/10.21228/M85T5M. RNA-seq and Metabolomics data are publicly available as of the date of publication. The analyzed non-targeted serum metabolomics dataset that supports the findings of this study is available as Table S2. All data reported in this study will be shared by the lead contact upon request.
- This paper does not report original code.
- Any additional information required to reanalyze the data reported in this paper is available from the lead contact, Professor Kirsi A. Virtanen (kirsi.virtanen@utu.fi), upon request.

EXPERIMENTAL MODEL AND SUBJECT DETAILS

Study participants

In total seventy-nine (79) study subjects were included in the study presented here. These data and biological samples were collected between 2009 and 2018 at the Turku PET Center during clinical studies exploring BAT metabolism in humans. The PET-CT imaging of BAT was performed using dynamic acquisition protocol.[22,24,25,34] There were 24 males and 55 females included in our cohort and, the group had an age range of 20–55 years and BMI ranging from 19 to 44 kg/m^2. All participants were clinically assessed before recruitment into the respective studies, with those presenting an overall healthy metabolic profile with no diabetes and/or cardiovascular diseases were included. The assessment and determination of a healthy metabolic health profile was based on available medical records, 2-h OGTT, electrocardiography (ECG) assessment, along with clinical lipid and hepatic enzyme levels in blood. All recruited study subjects provided written informed consent for volunteering in the clinical research studies. The study protocols were approved by the Ethics Committee of the Hospital District of Southwest Finland, and the studies were conducted according to the principles of the Declaration of Helsinki.

Table S1 shows the body composition and main clinical and metabolic variables of all the study participants included in the current report. Figure S1 shows a modified-Venn diagram for all of the major clinical assessments that have been made with the total number of participants in each of these clinical assessments; whereas overlap in the Venn-diagram shows the number of participants participating in both of these assessments.

Cell lines

Human Multipotent Adipose-Derived Stem (hMADS) cells were used for the *in-vitro* experimentation.[90] These cells were isolated from the white adipose tissue removed from the surgical scraps of infants undergoing surgery. The procedure was undertaken with the informed consent of the parents. All the methods were approved and performed following the guidelines and regulations of the Center Hospitalier Universitaire de Nice Review Board. These cells did not enter senescence while exhibiting a diploid karyotype, were non-transformed though expressing significant telomerase activity, showed no chromosomal abnormalities after 140 population doublings, and maintained their differentiation properties after 160–200 population doublings. hMADS cells were able to withstand freeze/thaw procedures, and their differentiation could be directed under different culture conditions into various lineages. In the experiments reported herein, hMADS cells were established from the prepubic fat pad of a 4-month-old male and used between passages 14 and 25.

METHOD DETAILS

Study design and methods

PET-CT imaging was carried out and blood samples were drawn after an overnight fast. The subjects were instructed to avoid consumption of alcoholic or caffeinated beverages for 12 h before the metabolic assessments. The subjects were also instructed to avoid strenuous physical activity 24 h before the study day. The subjects were placed in a supine position during the PET-CT scanning. The participants were scanned using PET-CT during cold-exposure using an individualized cooling protocol.[22,24] Subjects were classified as high-BAT and low-BAT based on substrate uptake rates; high-BAT glucose uptake rate of $\geq$3.0 μmol/100 g/min or NEFA uptake rate $\geq$0.7 μmol/100 g/min.[23] The cut-off value of 3.0 μmol/100 g/min glucose uptake rate is based on the equivalent of standardized uptake value (SUV) of FDG PET scan of 1.5 g/mL which has been the recommended SUV for the detection of BAT in BARCIST 1.0 criteria,[92] and NEFA uptake rate of 0.7 μmol/100 g/min is comparable in terms of energy content following complete oxidation to the glucose uptake rate value.

Biopsies and PET scanning protocol and analyses

Biopsy of supraclavicular adipose tissue was taken after obtaining written informed consent from the study participants. BAT depot in the supraclavicular region was localized with the aid of available imaging data (for example, MRI, cold-exposed [^{18}F]FDG PET, or cold-exposed [^{18}F]FTHA PET imaging). From the same incision site, subcutaneous adipose tissue was collected as a WAT sample.

The biopsies were obtained under local lidocaine-epinephrine anesthesia by a plastic surgeon at normal room temperature (approximately 22°C). Immediately after removal, the tissue samples were snap-frozen in liquid nitrogen.

PET-CT imaging

PET imaging of the supraclavicular region was performed with the subject supine positioning in the PET-CT scanner. Tissue glucose uptake rate was measured using [^{18}F]FDG radiotracer. Tissue blood perfusion was measured using [^{15}O]H_2O radiotracer. Tissue NEFA uptake rate was calculated using [^{18}F]FTHA. All PET scannings were performed using a dynamic acquisition protocol.[22,24]

RNA Isolation and mRNA gene expression from next-Generation sequencing

Deep-frozen adipose tissues (approx. 30–120 mg) were homogenized in 1 mL TRIsure (Bioline, London/UK) using a dispersing instrument (Ultra-Turrax D-1, Miccra GmbH, Muhlheim/Germany). RNA was prepared, further purified by spin columns (SV Total RNA Isolation System, Promega, Fitchburg WI/USA) and finally eluted in 50 mL water. The RNA concentration was determined photometrically (Nanodrop ND-1000, Peqlab, Erlangen/Germany). Samples were diluted to a concentration of 25–500 ng/mL, denatured for 2 min at 70°C and RNA integrity determined (Bioanalyzer 2100, Agilent Technologies, Santa Clara CA/USA). Sequencing libraries were prepared by enriching coding RNA to efficiently compensate for degradation (TruSeq RNA Access Coding Transcriptome, RS-301-2001, Illumina San Diego CA/USA) and libraries were sequenced (HiSeq 2500, Illumina).[24] The expression levels of the genes were expressed 'reads per 1kb transcript length per million mapped reads', RPKM. KEGG reference pathway for tryptophan[40] and nicotinamide[39] metabolism was used as a guideline for the determination of the genes of interest for a hypothesis-based statistical analysis.

Biochemical analyses

Fasting blood samples were utilized for measuring plasma concentrations of total cholesterol, HDL cholesterol and triglycerides with determined photometrical approach (ModularP800, Roche Diagnostics GmbH). The concentration of plasma low-density lipoprotein (LDL) was calculated using the Friedewald equation[93] during the visit before starting the PET scanning protocol.

Cell culture

The establishment and characterization of hMADS cells (human Multipotent Adipose-Derived Stem) was carried out according to the protocol developed by Rodriguez et al. (2005).[90] Cells were seeded at a density of 5000 cells/cm^2 in Dulbecco's Modified Eagle's Medium (DMEM) supplemented with 10% FBS, 15 mM HEPES, 2.5 ng/mL hFGF2, 60 mg/mL penicillin, and 50 mg/mL streptomycin. hFGF2 was removed when cells reached confluence. Cells were induced to differentiate,[94] in a serum-free medium, at day 2 post confluence (designated as day 0) in DMEM/Ham's F12 (1:1) media (NAM and tryptophan concentration 16.5μM and 44.2μM, respectively) supplemented with 10 μg/mL transferrin, 10 nM insulin, 0.2 nM triiodothyronine, 1 μM dexamethasone and 500 μM isobutylmethylxanthine for 4 days. Cells were treated between day 2 and 9 with 100 nM rosiglitazone (a PPARγ agonist), to enable white adipocyte differentiation. At day 14, the conversion of white to brite adipocytes was induced by rosiglitazone for 4 days (day 18). Media were changed every other day. NAM or tryptophan was added to the media at concentrations of 0.03 mM and 0.1 mM on day 18 for up to 6 h.

Isolation and analysis of RNA

These procedures followed MIQE standard recommendations.[95] Quantitative PCR (qPCR) were performed using SYBR qPCR premix Ex TaqII from Takara (Ozyme, France) and assays were run on a StepOne Plus ABI real-time PCR machine (PerkinElmer Life and Analytical Sciences, Boston). The expression of selected genes was normalized to that of 36B4 housekeeping gene and then quantified using the comparative-ΔCt method.

NAD^+ determination in human brite adipocytes

NAD^+ amount was measured from differentiated human brite adipocytes after 6 h treatment with vehicle, or NAM or tryptophan with the concentrations of 0.03 mM and 0.1 mM. Briefly, after washing with excess cold PBS, brite adipocytes were collected with cell scraper to Eppendorf tubes and pelleted with centrifugation. Excess PBS between floating adipocytes and pellets was removed, and tubes were stored at −80°C. NAD^+ amount was measured with Q-NAD Tissue/Cell NAD^+ and NADH assay kit (cat no: RUO_003) from NADMED according to the manufacturer's instructions. NAD^+ amount was normalized to protein amount of the assay cell pellet measured with BCA protein assay kit (Pierce, cat no: 23227).

MS-analysis of serum samples

Sample preparation: Fasting serum samples taken during the cold or RT exposures were stored at −80°C and thawed in an ice-water bath. Four hundred microliters of ice-cold acetonitrile (ACN) was pipetted to 96-well filter plates (Captiva ND Plate, 0.2 μm PP, Agilent Technologies, Santa Clara, CA, United States) after which 100 μL of plasma or quality control (QC) was added. The solution was mixed by pipetting up and down, filtrated by centrifugation (700 RCF, 4°C, 5 min) and collected to a 96-well plate (96 deep well plate natural, Thermo Scientific). QC was serum sample prepared by pooling an aliquot from all analyzed serum samples.

LC-MS: The samples were analyzed using ultra-high-performance liquid chromatography quadrupole time-of-flight mass spectrometry (UHPLC–qTOF-MS) system (Agilent Technologies), composed of a 1290 LC system, a Jetstream electrospray ionization (ESI) source, and a 6540 UHD accurate-mass qTOF spectrometer. All the samples were separated using reversed-phase (RP) chromatography and hydrophilic interaction (HILIC) chromatography. The sample tray was kept at + 10 °C during the analysis. The data acquisition software was the MassHunter Acquisition B.05.01 (Agilent Technologies).

For RP separation, a 2 μL extract aliquot was injected into the column (Agilent Zorbax Eclipse XDB-C18 Rapid Resolution HD 1.8 μm, 2.1 × 100 mm). Column temperature was 50°C and the flow rate was 0.4 mL/min. The mobile phases were composed of water with 0.1% (v/v) of formic acid (eluent A) and methanol with 0.1% (v/v) of formic acid (eluent B). The gradient used for the separation was as follows: 2 to 100% B in 10 min; 100% B from 10 min to 14.5 min; 100%–2% B, from 14.51 min to 16.5 min.

For HILIC, a 2 μL extract aliquot was injected into the column (Acquity UPLC BEH Amide column, 2.1 × 100 mm, 1.7 μm; Waters Corporation). The column temperature was kept at 45 °C and flow rate was 0.6 mL/min. The mobile phases consisted of 50% acetonitrile with 20 mM ammonium formate and 0.25% formic acid, pH 3 (Sigma-Aldrich) (eluent A) and 90% acetonitrile with 20 mM ammonium formate, 0.25% formic acid, pH 3. The separation gradient was as follows: 0 to 2.5 min, 100% B; 2.5 to 10 min, 100 → 0% B; 10 to 10.1 min, 0%–100% B; 10.1–12,5 min, 100% B. The sample tray was kept at 10°C. The gradient profile for HILIC separations: 0–2.5 min: 100% B, 2.5–10 min: 100% B → 0% B; 10–10.01 min: 0% B → 100% B; 10.01–12.5 min: 100% B.

MS conditions were as follows: Jetstream ESI source, operated in positive and negative ionization modes was used. For RP gas temperature was 325°C and flow 10 L/min and for sheath gas temperature was 350°C and flow rate 11 L/min. Nebulizer pressure was set as 3.103 bar (45 psig). Voltages for capillary, fragmentor, nozzle and skimmer were 3500 V, 100 V, 1000 V and 45 V, respectively. Mass range (m/z) of 65–1600 for data acquisition was used with a scan rate of 1.67 spectra/s. Abundance thresholds for MS and MS/MS were 150 and 5, respectively. The continuous mass calibration was used with *m/z* 922.009798 and *m/z* 121.05087300. For HILIC the MS-conditions were as for RP but the mass range (*m/z*) of 50–1600 was used for data acquisition.

MS/MS analysis for the identification process was performed for QC samples or for selected serum samples. For QC:s from precursor cycles the four most abundant ions were selected for MS/MS fragmentation with mass range of 65–1600 *m/z* with relative abundance of 0.01% (absolute 200 counts) and collision energies 10 V, 20 V or 40 V. The same ion was selected for the collision two times after which it was excluded for 0.25 min. For HILIC the MS-conditions were as for RP but the mass range (*m/z*) of 50–1600 for data acquisition was used. For single serum samples MS/MS analysis was performed in a targeted manner for selected ions using collision energies of 10 V and 20 V for HILIC and 10 V and 30 V for RP.

Identification: Metabolites were identified based on the in-house library built by running commercial standards using the same instrument and (experimental condition) with ion m/z tolerance of 10 ppm and spectral similarity (level I), experimental fragmentation spectra available in the literature or in public databases Metlin or Human Metabolome Database (HMDB) 4.0 with mass tolerance of 10 ppm a (level II) or with *in-silico* generated data in MS-FINDER software or in HMDB or with common fragmentation pattern denominator of the particular compound group, but the compound could not be identified due to the lack of reference spectra or other information (III). Fourth level (IV) included unknowns. For the identification levels see Sumner et al., (2007).[96]

QUANTIFICATION AND STATISTICAL ANALYSIS

For data analysis, metabolomics data were converted using Analysis Base File (ABF) Converter and signal detection (peak-picking) was performed with MS-DIAL software 3.52 (RIKEN Center for Sustainable Resource Science, http://prime.psc.riken.jp/Metabolomics_Software/index.html). The peak picking parameters were set as follows: MS1 tolerance was 0.01 Da, MS2 tolerance 0.025 Da, *m/z* range 0–1000 (small molecules), minimum peak amplitude 2000 signal counts, and mass slice width 0.1 Da. For peak smoothing linear weighted moving average was used; the smoothing level was 3 scans and minimum peak width 5 scans. The adduct ions for the positive mode were $[M + H]^+$, $[M + NH_4]^+$, $[M + Na]^+$, $[M + H\text{-}H_2O]^+$, $[M + H\text{-}2H_2O]^+$, $[M + K]^+$, $[2M + H]^+$ and for the negative mode $[M - H]^-$, $[M - H_2O - H]^-$, $[M + Cl]^-$, $[M + FA - H]^-$, $[2M - H]^-$, $[3M - H]^-$. For the peak alignment, an *m/z* tolerance of 0.025 Da and a retention time tolerance of 0.1 min were used. Gap filling by compulsion function was used to detect peak areas although no local peak maxima were found.

The metabolomics data were then preprocessed by separately conducting the following steps on each of the four analytical modes (HILIC negative, HILIC positive, RP negative and RP positive)[97] in R version 3.5.1.[98] Signals that were present in less than 80% of the samples in all of the study groups were removed. Signal quality was measured using error metrics defined in Broadhurst et al., (2018).[99] Signals were required to have a detection rate of at least 60% in the pooled QC samples. The remaining signals were corrected for the drift pattern caused by the LC-MS procedures. Regularized cubic spline regression was fit separately for each signal on the QC samples.[100] The performance of the drift correction was assessed using non-parametric, robust estimates of relative standard deviation of QC samples (RSD*) and D-ratio* as quality metrics. Drift correction was only applied if the value of both quality metrics decreased, leading to enhanced quality. Otherwise, the original signal was retained.

After the drift correction, low-quality signals were removed. Signals were kept if their RSD* was below 20% and their D-ratio below 40%. In addition, signals with classic RSD, RSD* and basic D-ratio all below 10% were kept. This additional condition prevents the removal of signals with very low values in all but a few samples. These signals tend to have a very high value of D-ratio*, since the median absolute deviation of the biological samples is not affected by the large concentration in a handful of samples, causing

the D-ratio* to overestimate the significance of random errors in measurements of QC samples. Thus, other quality metrics were applied, with conservative limit of 0.1 to ensure that only good-quality signals were kept this way.

The missing values in the good quality signals were imputed using random forest imputation implemented in the R package missForest version 1.4.[101] The out-of-bag (OOB) error estimates were low for all the modes, indicating high quality imputation. Signals were then normalized using inverse-rank normalization to approximate a normal distribution. QC samples were removed prior to imputation and normalization, to prevent them from biasing the procedures.

The normalized data matrices of each mode were combined for statistical analysis. This resulted in 7170 signals to be analyzed. Differential metabolites were identified using a linear mixed model fit separately for each metabolite using the lme4 R package version 1.1.20.[91] The metabolite level was used as the dependent variable, the group as a fixed factor and the subject ID as a random factor. The significance of the difference between the groups was tested using a t test on the regression coefficient based on Satterthwaite's denominator degrees of freedom as implemented in the lmerTest R package (version 3.1.0).[102] Results were adjusted for multiple comparisons using Benjamini-Hochberg false discovery rate (FDR). As an additional metric of effect size, fold change between the groups was calculated from the non-normalized dataset.

The comparisons of means for testing the differences between high- and low-BAT within the study groups (cold or RT) unpaired Student's t-test was performed. For the comparison of gene expression between BAT and WAT, paired Student's T test for normally distributed data or Wilcoxon rank-sum test for the non-normally distributed datasets. Correlations between variables were examined with Spearmen's rank correlation. For the data generated by *in-vitro* experimentation, statistical tests were performed with Prism (version 9, GraphPad) software. Outliers were identified using ROUT (Q = 1%) and excluded from the analysis. The normality of distributions was evaluated by the Shapiro–Wilk test. The significance of the differences was evaluated by analysis of variance (ANOVA) for normal distribution or Kruskal–Wallis test for nonnormal distribution. ANOVA was followed by the Fisher's Least Significant Difference (LSD) test, whereas the Kruskal–Wallis test was followed by the Uncorrected Dunn's test to assess differences of planned comparisons among groups. For other tests rather than global metabolomics, a p value of <0.05 was considered as statistically significant. Data are presented as mean ± SD, unless stated otherwise. N represents number of subjects, details of groups and statistical parameters can be found in the figure legends.